Noname manuscript No.
(will be inserted by the editor)

Effective behavior of cooperative and nonidentical molecular motors

Joe Klobusicky · John Fricks · Peter R. Kramer

Abstract Analytical formulas for effective drift and diffusivity are derived for an intracellular transport system consisting of a cargo attached to two cooperative but not identical molecular motors (for example, kinesin-1 and kinesin-2) which can each attach and detach from a microtubule. The dynamics of the motor and cargo in each phase are governed by stochastic differential equations, and the switching rates depend on the spatial configuration of the motor and cargo. This system is analyzed in a limit where the detached motors have faster dynamics than the cargo, which in turn has faster dynamics than the attached motors. The attachment and detachment rates are also taken to be slow relative to the spatial dynamics. Through an application of iterated stochastic averaging to this system, and the use of renewal-reward theory to stitch together the progress within each switching phase, we obtain explicit analytical expressions for the effective drift, diffusivity, and processivity of the motor-cargo system. Our approach accounts in particular for jumps in motor-cargo position that occur during attachment and detachment events, as the tracking variable makes a rapid adjustment due to the averaged fast scales. The analytical formulas are compared against stochastic simulations. For a certain parameter regime, we find that more effective transport by a team of

J. Klobusicky
Mathematical Science Department
Rensselaer Polytechnic Institute
110 8th Street, Troy, New York 12180, USA
Tel.: +123-45-678910
Fax: +123-45-678910
E-mail: klobuj@rpi.edu

John Fricks
School of Mathematical and Statistical Sciences
Arizona State University

P.R. Kramer
Mathematical Science Department
Rensselaer Polytechnic Institute

two different cooperative motors than for a team of two identical motors of either type.

Keywords Molecular motors · Stochastic averaging · Switched diffusion · Renewal-reward theory

1 Introduction

A biological cell during its interphase requires sufficiently fast transport of organelles and other compounds for its survival [1]. Transport through diffusion alone is often far too slow. To illustrate, a compound moving through pure diffusion in some neurons might take years to travel over the cell's length [2]. For eukaryotic organisms, intracellular trafficking of vesicles is instead governed by directed transport along a network of thin filaments, called microtubules. A vesicle and the molecular compound it encloses, collectively referred to as a cargo, travel along a microtubule by attaching to one or several molecular motors. The motors of interest to this paper, called kinesins, consist of two heads which attach to the microtubule, a tail which attaches to the cargo, and a coiled-coil tether connecting the heads and tail [3].

The motor-cargo attachment is generally found to be much more durable than the motor-microtubule attachment, so models of motor-cargo complexes typically assume the number of motors attached to a given cargo can be treated as a fixed constant N over the transport time scale of interest [4–9].

But the number of those N motors that are attached to microtubules and therefore actively engaged in transport does appear to fluctuate through dynamical attachment and detachment of the motors to and from the microtubule. In the present work, we contemplate the simplest scenario in which the motor-cargo complex is in the vicinity of a single microtubule. The state of the motor-cargo complex can then be classified in terms of which of its motors are attached to the microtubule, and therefore engaged in directed motion. Our model could also be formally applicable for a bundle of parallel microtubules with common polarity if they are spaced sufficiently closely that the progress of the cargo is not so sensitive to what particular set of microtubules the motors are attached. Rai et. al. in [10, Fig. S5] show experimental observations that approximating the multiple motors as all attached to a single microtubule could be consistent even for some situations in cell.

A cargo with two motors, for example, can fluctuate between three possible states while remaining connected to the microtubule: two states with one attached and one detached motor, and one state with two attached motors (Figure 1). One further state has both motors detached, after which we will consider the cargo to move away from the microtubule and terminate its run, though one could contemplate the motors remaining weakly bound and possibly sliding along the microtubule [11].

Microtubules are oriented with a + and - end, with the molecular motor kinesin always traveling from the - to + end [1] and the molecular motor dynein traveling in the opposite direction. This can result in "tug of war" scenarios and

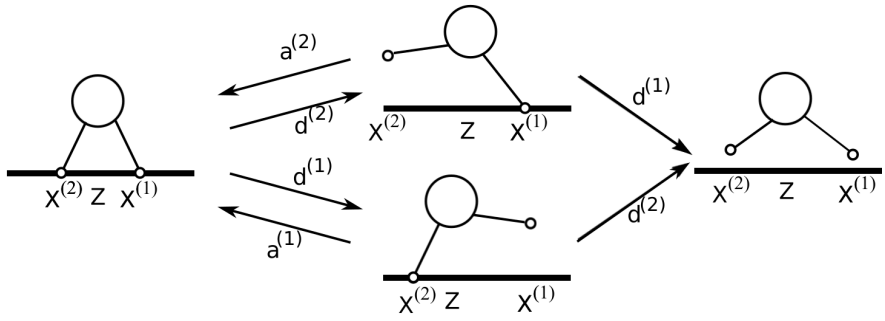

Fig. 1: Attachment and detachment from a microtubule for a system of two motors durably attached to a cargo. the The spatial positions along the microtubule for the motors are denoted $X^{(1)}$, and $X^{(2)}$, and for the cargo by Z. From a state with two attached motors (left), each motor i can detach with a rate $d^{(i)}$ depending on the current spatial configuration. From a state with one attached and one detached motor (center), the detached motor i can (re)attach with a constant rate $a^{(i)}$, or the attached motor i' can also detach at a configuration-dependent rate $d^{(i')}$, terminating the run on the microtubule.

bidirectional transport for ensembles including such antagonistic motors [12]. Our focus here is on cooperative transport of a cargo by possibly different motor types which each move, when considered in a single motor complex, in the same direction on the microtubule, such as two different types of motors from the kinesin superfamily.

As we wish to contemplate the possibility of the motors being different types of kinesin, the motor labelling is relevant and we distinguish between the two states with one motor attached. This is in contrast to models with N identical motors attached, which can be classified more compactly in terms of simply the number of those motors which are currently attached to a microtubule [13]. For multiple motor complexes, we are interested in calculating how statistics such as run lengths and effective speeds depend on the properties of the individual motors. Comparisons of statistics between motor complexes are sometimes counterintuitive. For instance, it has been observed in [14] that heterogeneous motor complexes of kinesin-1 and kinesin-2 have longer run lengths than pure systems consisting only of kinesin-1. However, statements such as this become less paradoxical when considering that effective quantities for multiple motor systems are dependent upon a variety of physical parameters, often interacting in complex ways. Indeed, while kinesin-2 is about half as fast as kinesin-1 and detaches more readily under load, it also appears to reattach to microtubules four times more quickly than kinesin-1 [14].

A number of properties of some individual motors, acting in isolation, have been obtained from in vitro experiments with molecular tweezers, in which a polystyrene bead, serving as a cargo, is attached to a motor, and directed along

a microtubule with an applied laser trap force. Under this setting, several motor properties can be measured, particularly their speed, diffusivity, and detachment rate as a function of the applied laser trap force [15–21]. The above experimental work can be used as a basis for parameterizing biophysically mechanistic models for individual motors in theoretical models exploring their interactions [5, 22].

For the purpose of experimentally measuring the interaction of molecular motors, and in particular for motivation for and comparison against theoretical models, an important recent experimental development is to use DNA origami for cargo, which specifies closely arranged handle sites onto which specified motor types attach. The attachment of the motors to the cargo is typically treated as permanent during an experiment, and motor-cargo attachment is thought to also be long-lived for natural cargos in vivo relative to time scales of association of the motor-cargo complex with microtubules. The actual engagement of motors with microtubules cannot be resolved, so particularly when not using engineered motor-attachment constructs, the number of relevant motors of various types attached to an observed cargo with a particular microtubule must typically be statistically inferred, sometimes using simple theoretical models.

Experiments and numerical simulations of biophysical models show that the transport of a cargo by a team of cooperative motors depends both quantitatively and qualitatively on the properties of the individual motors. For example, teams of dynein molecules are understood, relative to teams of kinesin molecules, to better coordinate in generating larger forces and longer run lengths due to three key characteristics of the individual motors: the shape of the force-velocity relation, catch bond behavior in detachment rate as a function of force, and the ratio of the force-scale of detachment to that of stall. More recent work finds that in fact the stall force and velocity of a team of two dyneins also depends on the type of adaptors present. Numerical simulations of find that the properties of kinesin teams is mostly dependent on the attachment/detachment rates of the motors from the microtubule, and not so sensitive to other structural and mechanical properties compared the teaming of conventional kinesin (kinesin-1) motors with another family of kinesin (Ncd aka kinesin-14), and found the latter was able to markedly increase their run length in teams up to 4 motors. The key difference between the two families of kinesin leading to the different teaming effectiveness was traced to the relative strong diffusion of Ncd (kinesin-14), which teaming was able to significantly reduce.

The main modeling framework from which we base our paper is from McKinley et al. [23], where cargo transport statistics were examined for cooperative ensembles of identical motors that are treated as permanently attached to the microtubule. The coupled spatial dynamics of the motor and cargo position are expressed as a system of continuous stochastic differential equations (SDEs) which are viewed as a coarse-graining of discrete stepping model. In Section 2, we will extend this model in two ways: 1) allowing the motors to be distinct, but still cooperative, and 2) allowing the motors to attach and

detach from the microtubule. The modification of the spatial dynamics is presented in Subsection 2.1, resulting in a system of SDEs (1)-(5) with the motor dynamics depending on both the motor label and whether the motor is attached or detached. The cargo and detached motor dynamics are modeled as overdamped point particles responding to spring forces from the motor-cargo tether and driven by stochastic terms representing thermal fluctuations. On the other hand, as in [23], the attached motors dynamics are governed by a nonlinear force-velocity relation together with stochastic terms arising from the nonequilibrium stepping process.

Punctuating the continuous evolution of the motor-cargo dynamics is the attachment or detachment of motors from the microtubule. In Subsection 2.1, we present our Markovian model of switching times. Attachment rates are rather difficult to quantify experimentally, and we simply adopt the common approach of modeling them as constant (as in a homogenous Poisson process model). The detachment rates, on the other hand, will be taken as functions of the applied force on the attached motor, which is itself a stochastic process induced by the stochastic spatial dynamics. Mathematically, then, the detachment process is more akin to a Cox process. The class of functions we consider for detachment rates is general enough to include the most common cases seen in previous works, including constant [24] and exponential [18,22,25] functions. Transitions between attached and detached states have been modeled as continuous time Markov chains in the case of identical motors [13,26,27] with constant switching rates depending on the number of attached and detached motors. Our model allows for nonidentical motors, which increases the state space of possible attachement and detachment configurations. Similar to the discrete-space models discussed in [26,27], our transition rates depend on relative motor positions, but now must consider motor types. Moreover, our model does not make the popular assumption that the cargo is always in mechanical equilibrium with the motors nor the further mean-field approximation that all motors feel a perfectly shared load from the cargo. Stochastic fluctuations of cargo and motor positions have been shown to significantly alter the mean-field predictions, at least for small teams of motors, and experimental observations do not support the load-sharing assumption in teams of two kinesin-1.

The analysis of our model will proceed by an extension of the asymptotic analysis developed in [23], based on the cargo dynamics being taken as fast relative to the dynamics of the motors attached to the microtubule. Extending this nondimensionalization to our setting of nonidentical motors which attach and detach from the microtubule in Section 3.1, we further motivate taking the detached motor dynamics to be faster than the cargo (due to their relative size), and the attachment and detachment processes as slow compared to the dynamical time scale of attached motors. We set up an asymptotic analysis which formalizes these separations of time scales, with the further assumption that the parameters for different motor types do not vary drastically (which seems to be reasonable for kinesin 1 versus kinesin 2, for example, [18]). We proceed in Subsection 3.2 to apply stochastic averaging successively over the

unbound motor positions and the cargo position to obtain effective dynamics and effective detachment rates based only on the positions and identities of the attached motors. The analysis thus far applies to N cooperative but possibly not identical motors, and in fact does not require a time scale separation assumption between the attached motor dynamics and attachment/detachment dynamics. Further analytical progress can be achieved for the case of $N = 2$ motors if we adopt this time scale separation to homogenize the effective dynamics obtained from the stochastically averaged equations within each interval between attachment or detachment. The results from the homogenization are presented in Section 3.3, with the derivation in Appendix C.

Finally, to obtain effective velocity, diffusivity, and processivity statistics, we apply in Section 5 a central limit theorem for renewal-reward processes to the progress made by the motor-cargo complex over several cycles of attachment and detachment events. [28] appealed to similar renewal theory arguments for a discrete semi-Markov stepping model to compute effective statistics for motor head stepping from a chemomechanical cycle model, and applied this framework to describe the effective dynamics of a ParB protein complex that moves along a track of ParA proteins in a manner similar to molecular motors which "burn" the track as they progress. These transport properties are all expressed in terms of explicit formulas involving the parameters governing the motor and cargo dynamics. In a broad sense, our strategy of combining asymptotic arguments regarding separation of time scales and renewal-reward calculations to obtain these explicit formulas mirrors that of Lawley for the case of identical cooperative motors with force-independent detachment rates. But the implementation of these ideas differ in some details which we will discuss in the conclusion (Section 7). Computational model compared against averaging assumptions are provided in Section 6. We conclude with a discussion in Section 7.

2 Models of evolution and switching

For a fixed number of attached and detached motors, we model the transport of a motor and cargo system through a system of SDEs. Similar to [23], we coarse-grain over this discrete stepping and model this motion as a one-dimensional continuous process along the direction of the microtubule, neglecting transverse fluctuations. The locations of N motors over time t are denoted by $X^{(i)}(t) \in (-\infty, \infty)$, $i = 1, \ldots, N$. During a realization of the stochastic process, a motor will change its state from time to time. We will denote the ith motor's state at time t as $B^{(i)}(t) \in \{0, 1\}$, where 0 and 1 denote detached and attached states, respectively. The switching between motor states will be governed by a continuous-time Markov chain model, with switching rates due to attachment and detachment depending on the distances between the motors and cargo. All motors in the system are assumed to remain attached to a single cargo, with a position of $Z(t)$.

2.1 Drift and diffusion of nonidentical motors

For a motor system with N motors the governing equations take the autonomous form

$$dX^{(i)}(t) = \left(\mu_d^{(i)}(X^{(i)}(t), Z(t))dt + \sqrt{2k_BT/\gamma_m^{(i)}}dW^{(i)}(t)\right)(1 - B^{(i)}(t)) \quad (1)$$

$$+ \left(\mu_a^{(i)}(X^{(i)}(t), Z(t))dt + \sigma^{(i)}dW^{(i)}(t)\right)B^{(i)}(t) \quad 1 \le i \le N, \quad (2)$$

$$\gamma dZ(t) = -\sum_{j=1}^{N} F^{(j)}(X^{(j)}(t) - Z(t))dt - F_T dt + \sqrt{2k_BT\gamma}dW_z(t). \quad (3)$$

with drift coefficients $\mu_a^{(i)}, \mu_d^{(i)} : \mathbb{R}^2 \to \mathbb{R}$ for the motors satisfying

$$\mu_a^{(i)}(x, z) = v^{(i)}g(F^{(i)}(x - z)/F_s^{(i)}), \quad (4)$$

$$\mu_d^{(i)}(x, z) = F^{(i)}(x - z)/\gamma_m^{(i)}. \quad (5)$$

A table of the parameters and their roles can be found in Table 1. We next briefly summarize the meaning of the model equations (1)-(5); more details can be found in [23].

If $B^{(i)}(t) = 1$, equation (1) describes an attached motor with position $X^{(i)}(t)$. The restorative force in (4) results from the stretching of the coiled-coil tether that connects the motor head and tail. For simplicity in the analysis to follow, we model the force for this tether for motor i by the Hookean spring relation $F^{(i)}(y) = -\kappa^{(i)}y$, where y is the longitudinal displacement from the cargo to the motor, and $\kappa^{(i)}$ is the effective spring constant for the ith motor. The analysis for nonlinear motors is similar, and is discussed in Appendix B. The nondimensional force velocity relation $g : \mathbb{R} \to \mathbb{R}$ is multiplied by an unencumbered velocity $v^{(i)}$ to produce an instantaneous expected velocity. The argument of g measures the ratio between the spring force and the motor's stall force $F_s^{(i)}$, or the opposing force needed from the cargo to anchor a motor. To agree with the definitions of $v^{(i)}$ and $F_s^{(i)}$, g must satisfy $g(0) = 1$ and $g(1) = 0$. Random effects are modelled by independent Brownian motions $W^{(i)}(t)$, with an effective motor diffusion of $\frac{1}{2}(\sigma^{(i)})^2$.

When $B^{(i)}(t) = 0$, the equation for the position of an detached motor $X^{(i)}(t)$ in (1) is an overdamped Langevin equation for a particle with a friction constant $\gamma_m^{(i)}$, and spring constant $\kappa^{(i)}$. The fraction constant $\gamma_m^{(i)}$ was computed with the Stokes Einstein relation $\gamma_m^{(i)} = 6\pi a\eta$ for a spherical cargo of radius 500 nm in water, with a fluid viscosity of 10^{-9} pNs/nm^2. The Brownian motions $W^{(i)}(t)$ are independent of each other, and also of the Brownian motion $W_z(t)$ driving the cargo. Finally, the constant k_BT is the Boltzmann constant multiplied by temperature.

The equation for cargo position $Z(t)$ in (3) also follows an overdamped Langevin equation with friction constant γ (also calculated using the Stokes Einstein law with $a = 50$ nm), but differs from that of detached motors in two

ways. First, the cargo is subject to to spring forces from each of the N motors. Second, we also account for a possible constant applied laser trap force F_T.

We model the transition between attachment configurations with varying numbers of attached and detached motors with a Markov chain switching model. See Table 1 for a list of typical attachment/detachment values. The attachment of motors is modeled by a homogeneous Poisson process, with each detached motor having an attachment rate of $a^{(i)}$. As in most theoretical work (CITE Lipowsky and others), we take the attachment rates to be independent of the configuration of the motor-cargo complex. The attachment rate of a motor can naturally be expected to be somewhat different when at least one other motor on the same cargo is also attached to a microtubule than when none are, as does seem to be indicated experimentally [**?**]. As we do not model the attachment of the motor-cargo complex from a state of no attached motors, the attachment rate we require is the one where at least one other motor on the same cargo is currently attached to a microtubule. We therefore take our parameter value for $a^{(i)}$ in Table 1 from recent experimental measurements in this setting, rather than the conventional estimate in modeling work [13] based on single-kinesin attachment rates.

Detachment rates are determined through the force dependent function

$$d^{(i)}(F) = d_0^{(i)} \Upsilon^{(i)}(F/F_d^{(i)}). \tag{6}$$

Here, the parameter $F_d^{(i)}$ is a scale force, and $\Upsilon^{(i)}$ satisfies $\Upsilon(0) = 1$, so that $d_0^{(i)}$ is the detachment rate under no external force. A common choice of $\Upsilon^{(i)}$, following the theory of Bell [29], is an exponential function (see [6,22], for instance), and will be used in the simulations of Section 6. The total force $F^{(i)}(t)$ felt on motor i at time t consists of the cargo spring force, which is

$$F^{(i)}(t) = \kappa^{(i)}(X^{(i)}(t) - Z(t)). \tag{7}$$

Note that since we are only modeling the motor-cargo dynamics along the microtubule direction, our detachment rate model correspondingly depends only on the longitudinal force. Forces are dependent on motor and cargo position, which implies that $F(t)$, and thus $d(F(t))$, are random. The resulting model for detachment thus amounts to a Cox process, a generalization of a Poisson process in which the intensity function may be a random process (see [30] for an introduction).

From the additivity of Poisson rates, a system with N_u attached motors has a constant total attachment rate of $\sum_{i:B^{(i)}=0} a^{(i)}$.

Under constant detachment rates $d^{(i)}$, $i = 1, \ldots, N$, which occur when $\Upsilon^{(i)}$ is a constant function, switching between states is a homogeneous, continuous time, finite state Markov chain, with an average time $\tau(\mathbf{S})$ spent in a state $\mathbf{B} = (B^{(1)}, \ldots, B^{(N)})$ given by

$$\tau(\mathbf{S}) = \frac{1}{\sum_{j=1}^{N}(1 - B^{(j)})a^{(j)} + \sum_{j=1}^{N} B^{(j)} d^{(j)}}. \tag{8}$$

Table 1: Typical values for kinesin-1 in water-like environments. Values of parameters which differ for kinesin-2 (specifically, KIF3A/B) are in bold with parentheses. [32–35, 20, 21, 19]

Parameter	Description	Typical values
F_s^i	Motor stall force	4.7 pN [5] ~~(MEMO: 5 pN in Mogilner? In cell?)~~
k_BT	Boltzmann constant by temperature	4.1 pN nm
$\kappa^{(i)}$	Neck linker spring constant	0.25 pN/nm [36] ~~(CITE Furuta)~~
$v^{(i)}$	Unencumbered motor velocity	790 nm/s, (**500 nm/s**) [18]
γ	Cargo friction	1×10^{-5} pN s/nm [23]
$\gamma_{m,i}$	Motor friction	1×10^{-6} pN s/nm
$(\sigma^{(i)})^2$	Effective motor diffusion	5000 nm^2/s (**1500 nm^2/s**)[32, 18]
F_T	Optical trapping force	-6 to 20 pN [16] ~~(CITE Milic)~~
$a^{(i)}$	Motor attachment rate	4/s (**16/s**) [14]
$d_0^{(i)}$	Zero force attached motor detachment rate	.66/s (**2.75/s**) [18]
F_d^i	Force scale for detachment	1.78 pN (**2.41 pN**) [18]

For more complicated detachment rates, the average time until either first detachment or attachment admits no explicit solutions. As we will see in Section 4, however, under a slow switching regime, we may approximate detachment rates by constants $\bar{d}^{(i)}$ through averaging over possible motor-cargo configurations. This is in contrast to the quasi-steady state model studied by Bressloff and Newby, in which transitions between states are considered fast compared to motor velocities [31].

3 Nondimensionalization and averaging

3.1 Nondimensionalization

For the purposes of reducing the number of parameters in a motor-cargo system, we perform a nondimensionalization of (1)-(5), adapting the nondimensionalizaton in McKinley et. al [23] for the case of identical cooperative motors. To not only nondimensionalize but normalize the variables for the asymptotic reduction exploiting time scale disparities [37, 38], a reference time scale of γ/κ and a reference length scale of $\sqrt{2k_BT/\kappa}$ was taken in the nondimensionalization. These characterize the nominal fluctuation dynamics of the cargo, so the resulting nondimensional equations are normalized to order unity for the cargo, and manifest the relatively slow dynamics of the attached motors.

With nonidentical motors, it will become necessary to use an average of motor parameters in order to maintain consistent scalings for all motors. Toward this end, denote

$$\bar{\kappa} = \sum_{j=1}^{N} \kappa^{(j)}/N, \quad \tilde{\kappa}^{(i)} = \kappa^{(i)}/\bar{\kappa}. \tag{9}$$

Under the change of coordinates $\tilde{t} = \bar{\kappa}t/\gamma$, and

$$\tilde{X}^{(i)}(\tilde{t}) = \frac{X^{(i)}(\gamma\tilde{t}/\bar{\kappa})}{\sqrt{2k_BT/\bar{\kappa}}}, \qquad \tilde{Z}(\tilde{t}) = \frac{Z(\gamma\tilde{t}/\bar{\kappa})}{\sqrt{2k_BT/\bar{\kappa}}}, \tag{10}$$

equations (2) and (3) may be written in nondimensional form

$$d\tilde{X}^{(i)}(\tilde{t}) = \left(\epsilon^{(i)} g(s^{(i)}(\tilde{X}^{(i)}(\tilde{t}) - \tilde{Z}(\tilde{t}))d\tilde{t} + \sqrt{\hat{\rho}^{(i)}\epsilon^{(i)}}dW^{(i)}(\tilde{t})\right) B^{(i)}(t) \tag{11}$$
$$+ \left(-(\Gamma^{(i)})^{-1}\tilde{\kappa}^{(i)}(\tilde{X}^{(i)}(\tilde{t}) - \tilde{Z}(\tilde{t}))d\tilde{t} + (\Gamma^{(i)})^{-1/2}\, dW^{(i)}(\tilde{t})\right)(1 - B^{(i)}(t)), \quad 1 \le i \le N,$$

$$d\tilde{Z}(\tilde{t}) = \left(\sum_{j=1}^{N} \tilde{\kappa}^{(j)}(\tilde{X}^{(j)}(\tilde{t}) - \tilde{Z}(\tilde{t})) - \tilde{F}_T\right) d\tilde{t} + dW_z(\tilde{t}). \tag{12}$$

The nondimensional attachment and detachment rates are now $\tilde{a}^{(i)} = a^{(i)}\gamma/\bar{\kappa}$ and $\tilde{d}^{(i)} = d^{(i)}\gamma/\bar{\kappa}$. Under this nondimensionalization, the detachment rate (6) then becomes (expressed now as a stochastic process in time):

$$\tilde{d}^{(i)}(\tilde{t}) = \tilde{d}_0^{(i)}\Upsilon(u^{(i)}(\tilde{X}^{(i)}(\tilde{t}) - \tilde{Z}(\tilde{t})). \tag{13}$$

A listing of nondimensional parameters introduced in Eqs. (11)-(13) and their typical values are provided in Table 2.

3.2 Multiscale Averaging

By comparing magnitudes of drift coefficients, we are now able to identify fast and slow variables. For systems with multiple scales, a common method of dimension reduction averages out fast variables by considering their stationary distributions against fixed values of slow variables (see [39] for multiple examples). In our case, from Table 2 and Eqs. (11) and (12), we observe that a plausible asymptotic ordering for the nondimensional parameters is: $\tilde{a}^{(i)} \sim \tilde{d}^{(i)} \ll \epsilon^{(i)} \ll 1 \ll (\Gamma^{(i)})^{-1}$. That is, the dynamics for detached motors are faster than those for the cargo, which in turn are faster than those for attached motors, which in turn are faster than the attachment and detachment processes. We by no means claim this asymptotic ordering is well satisfied for all molecular motors, or for kinesin-1 under all conditions, but simply that the assumptions on which our asymptotic simplification is based is at least plausible based on the kinesin-1 data we have drawn from the literature, summarized in nondimensional form in Table 2. Also, for mixtures of motors, while we allow the attachment, detachment, and unencumbered velocities to differ, we assume the parameters in each group are of the same order of magnitude in our asymptotic ordering ($\tilde{a}^{(i)} \sim \tilde{a}^{(i')} \sim \tilde{d}^{(i)} \sim \tilde{d}^{(i')}$, $\epsilon^{(i)} \sim \epsilon^{(i')}$ for all $1 \le i, i' \le N$). We remark that a similar hierarchy of time scales was considered in the context of the stepping of the two heads of a kinesin motor attached to a cargo in [**?**], where the detached head was taken to move quickly

relative to the cargo, while the cargo dynamics were taken as fast relative to the time scale of motor stepping.

While the focus for this paper will mainly be for two motor systems, it is possible to write averaged formulas for both detached motor and cargo positions under a generic system of N motors. Fixing a time $t \geq 0$ and motor index i, if $B^{(i)}(t) = 0$, we may regard the distribution of the detached motor $\tilde{X}^{(i)}(t)$ as approximately that of the quasistationary distribution $p_{\tilde{X}^{(i)}}$ under fast detached phase dynamics ($B^{(i)}(t) = 0$ in Eq. 11), with the slower cargo variable $\tilde{Z}(\tilde{t})$ held at a fixed value $\tilde{z}$. This is the Gaussian PDF

$$p_{\tilde{X}^{(i)}|\tilde{Z}}(\tilde{x}|\tilde{z}) = \sqrt{\frac{\tilde{\kappa}^{(i)}}{\pi}} \exp\left(-\tilde{\kappa}^{(i)}(\tilde{x}-\tilde{z})^2\right), \tag{14}$$

and all detached motor positions are independent when the cargo position $\tilde{Z}(\tilde{t}) = \tilde{z}$ is held fixed. Similarly, by fixing the positions of the slow attached motors, an approximation of the distribution of the faster cargo position is the quasi-stationary distribution $p_{\tilde{Z}|\tilde{\mathbf{X}}^{(a)}}$ of (12) with the states of all motors and the positions of the attached motors held at fixed values, which is another Gaussian of the form

$$\begin{aligned} &p_{\tilde{Z}|\tilde{\mathbf{X}}^{(a)},\mathbf{B}}(\tilde{z}|\mathbf{x},\mathbf{b}) \qquad (15)\\ &= \sqrt{\frac{\sum_{j=1}^N b^{(j)}\tilde{\kappa}^{(j)}}{\pi}} \exp\left[-\left(\sum_{j=1}^N b^{(j)}\tilde{\kappa}^{(j)}\right)\left(\tilde{z} - \left[\frac{\sum_{i=1}^N b^{(j)}\tilde{\kappa}^{(j)}\tilde{x}^{(j)} - \tilde{F}}{\sum_{i=1}^N b^{(j)}\tilde{\kappa}^{(j)}}\right]\right)^2\right], \end{aligned}$$

where $\mathbf{x} = (x^{(1)}, x^{(2)}, \ldots, x^{(N)})$ and $\mathbf{b} = (b^{(1)}, b^{(2)}, \ldots, b^{(N)})$ parameterize, respectively the positions and states of all N motors. Note that the above formula for the quasi-stationary distribution of the cargo does not actually depend on the positions of the detached motors (indices i for which $b^{(i)} = 0$), as these are fast relative to the cargo, and so are treated as already averaged out on the cargo time scale. This is why we denote the fixed variable as $\mathbf{X}^{(a)}$, though we write the quasi-stationary distribution formally as a function of all motor positions to keep notation simple. Moreover, the averaging of the detached motors does not affect the cargo dynamics to leading order due to the simple linear stochastic model (12) for the cargo dynamics. In the case of full motor attachment ($b^{(i)} = 1$ for all i), the average position for the cargo is a weighted average of motor positions shifted by the nondimensional trap force divided by the number of motors, $\tilde{F}/N$. We will often refer to (15) in the specific case of systems with $N = 2$ motors. With one out of the two motors

attached,

$$p_{\tilde{Z}|\tilde{\mathbf{X}}^{(a)},\mathbf{B}}(\tilde{z}|(\tilde{x}^{(1)},\tilde{x}^{(2)}),(1,0)) = \sqrt{\frac{\tilde{\kappa}^{(1)}}{\pi}}\exp\left[-\tilde{\kappa}^{(1)}\left(\tilde{z}-\tilde{x}^{(1)}+\frac{\tilde{F}}{\tilde{\kappa}^{(1)}}\right)^2\right], \tag{16}$$

$$p_{\tilde{Z}|\tilde{\mathbf{X}}^{(a)},\mathbf{B}}(\tilde{z}|(\tilde{x}^{(1)},\tilde{x}^{(2)}),(0,1)) = \sqrt{\frac{\tilde{\kappa}^{(2)}}{\pi}}\exp\left[-\tilde{\kappa}^{(2)}\left(\tilde{z}-\tilde{x}^{(2)}+\frac{\tilde{F}}{\tilde{\kappa}^{(2)}}\right)^2\right],$$

and with both motors attached,

$$p_{\tilde{Z}|\tilde{\mathbf{X}}^{(a)},\mathbf{B}}(\tilde{z}|(\tilde{x}^{(1)},\tilde{x}^{(2)}),(1,1)) = \sqrt{\frac{2}{\pi}}\exp\left[-2\left(\tilde{z}-\frac{\tilde{\kappa}^{(1)}\tilde{x}^{(1)}+\tilde{\kappa}^{(2)}\tilde{x}^{(2)}}{2}+\frac{\tilde{F}}{2}\right)^2\right]. \tag{17}$$

Our nondimensionalization set the time scale to be order unity for the cargo, so the dynamics of the slower attached motors appears weak on this time scale (ord($\varepsilon^{(i)}$) drift and diffusivity for attached motors i, with $\varepsilon^{(i)} \ll 1$). Thus, to see nontrivial attached motor dynamics, we must go to a longer time scale

$$\tilde{t} = \bar{t}/\bar{\epsilon}, \quad \bar{\epsilon} = \sum_{j=1}^{N}\epsilon^{(j)}/N, \tag{18}$$

over which the cargo now appears $O((\bar{\epsilon})^{-1})$ fast and equilibrates quickly relative to changes in attached motor position. From stochastic averaging theory (see [40,41]), we can approximate the attached motor positions on this time scale $\tilde{X}^{(i)}(\bar{t}/\bar{\epsilon})$ by an averaged stochastic process $\bar{X}^{(i)}(\bar{t})$ satisfying the system of SDEs

$$d\bar{X}^{(i)}(\bar{t}) = \bar{g}^{(i)}(\{\bar{X}^{(i)}\}_{i=1}^{N}(\bar{t});\{B^{(i)}\}_{i=1}^{N})d\bar{t} + \sqrt{\rho^{(i)}}dW^{(i)}(\bar{t}), \quad \rho^{(i)} = \frac{\epsilon^{(i)}}{\bar{\epsilon}}\hat{\rho}^{(i)}, \tag{19}$$

with an effective drift obtained by averaging over the quasi-stationary distribution of the cargo:

$$\bar{g}^{(i)}(\mathbf{x};\mathbf{s}) = \frac{\epsilon^{(i)}}{\bar{\epsilon}}\int_{\mathbb{R}} g(s^{(i)}(\tilde{x}^{(i)}-\tilde{z}))p_{\tilde{Z}|\tilde{\mathbf{X}}^{(a)},\mathbf{B}}(\tilde{z}|\mathbf{x},\mathbf{b})d\tilde{z}. \tag{20}$$

Note the averaged dynamics of the attached motors in Eq. (19) are coupled directly to each other, through the averaging out of the cargo variable to which they are explicitly coupled in (11). The averaged drift $\bar{g}^{(i)}$ ostensibly depends on all motor positions, but it actually is independent of the detached motor positions because the same is true of $p_{\tilde{Z}|\tilde{\mathbf{X}}^{(a)},\mathbf{B}}$ in Eq. (15). Bouzat [42] proposes alternatively to coarse-grain the effects of the cargo fluctuations on the effective velocity of motors through an exponential time-averaging of the force felt from the cargo. This should give equivalent results to the more straightforward

stochastic averaging used here for the "robust" regime of averaging time scales advocated in [42].

Continuing with our assumption that the detachment process is slow compared to the time scale of motor motion ($\tilde{d}^{(i)} \ll \epsilon^{(i)}$), we may also obtain an averaged detachment rate $\bar{d}^{(i)}(\mathbf{x})$ for each motor i:

$$\bar{d}^{(i)}(\mathbf{x}, \mathbf{s}) = \tilde{d}_0^{(i)} \bar{\epsilon} \int_{\mathbb{R}} \Upsilon \left(u^{(i)} \left(\tilde{x}^{(i)} - \tilde{z} \right) \right) p_{\tilde{Z}|\tilde{\mathbf{X}}^{(a)},\mathbf{B}}(\tilde{z}|\mathbf{x}, \mathbf{b}) d\tilde{z}. \tag{21}$$

When a detached motor attaches, its attachment position is taken to be drawn from the quasi-stationary distribution of the detached motors, given fixed positions of the attached motors. This follows from our modeling of the attachment process as independent of spatial configuration in the present work; we discuss this assumption relative to other attachment modeling approaches in the literature in Section 7. [42] place attaching motors uniformly at random over the region of the microtubule where the motor-cargo tether is unstretched; this would be roughly consistent with our approach when the linear spring is modified to give no resistance to compression below a rest length (see Appendix (A)). Because of the assumed time scale separation, the relative position of the detached motors and the cargo is independent of the relative position of the cargo and the attached motors, and these are governed by the respective Gaussian quasi-stationary distributions (14) and (16). The quasi-stationary distribution of the position of the detached motors for fixed positions of the attached motors is therefore obtained by composing these Gaussian quasi-stationary distributions, leading to a convolution giving rise to a Gaussian distribution as well. In the simple case of $N = 2$ motors with exactly one of the two motors currently attached, the probability densities for the attachment position of the detached motor would be:

$$p^{(a)}_{\tilde{X}^{(2)}}(x'|(\tilde{x}^{(1)}, \tilde{x}^{(2)}), (1,0)) = \int_{\mathbb{R}} p_{\tilde{X}^{(i)}|\tilde{Z}}(x'|\tilde{z}) p_{\tilde{Z}|\tilde{\mathbf{X}}^{(a)},\mathbf{B}}(\tilde{z}|(\tilde{x}^{(1)}, \tilde{x}^{(2)}), (1,0)) d\tilde{z} \tag{22}$$

$$= \sqrt{\frac{\tilde{\kappa}^{(1)}\tilde{\kappa}^{(2)}}{2\pi}} \exp\left(-\frac{\tilde{\kappa}^{(1)}\tilde{\kappa}^{(2)}}{2} \left(x' - \tilde{x}^{(1)} + \frac{\tilde{F}}{\tilde{\kappa}^{(1)}} \right)^2 \right), \tag{23}$$

$$p^{(a)}_{\tilde{X}^{(1)}}(x'|(\tilde{x}^{(1)}, \tilde{x}^{(2)}), (0,1)) = \sqrt{\frac{\tilde{\kappa}^{(1)}\tilde{\kappa}^{(2)}}{2\pi}} \exp\left(-\frac{\tilde{\kappa}^{(1)}\tilde{\kappa}^{(2)}}{2} \left(x' - \tilde{x}^{(2)} + \frac{\tilde{F}}{\tilde{\kappa}^{(2)}} \right)^2 \right). \tag{24}$$

For the general case of N motors, the attachment position of a currently detached motor i would have a Gaussian probability distribution with mean

$$\frac{\sum_{j=1}^{N} b^{(j)} \tilde{\kappa}^{(j)} \tilde{x}^{(j)} - \tilde{F}}{\sum_{j=1}^{N} b^{(j)} \tilde{\kappa}^{(j)}}$$

Table 2: Nondimensional groups and typical values for kinesin-1 and kinesin-2 (in bold text with parentheses).

Group	Definition	Typical value
$\epsilon^{(i)}$	$\frac{v^{(i)}\gamma}{\sqrt{2k_BT\bar{\kappa}}}$	$4.7\times10^{-3}, (\mathbf{3.0\times10^{-3}})$
$s^{(i)}$	$\frac{\kappa^{(i)}}{F_s}\sqrt{\frac{2k_BT}{\bar{\kappa}}}$	0.2
$\tilde{F}$	$\frac{F_T}{\sqrt{2k_BT\bar{\kappa}}}$	$1-10$
$\hat{\rho}^{(i)}$	$\frac{(\sigma^{(i)})^2\sqrt{\bar{\kappa}}}{v^{(i)}\sqrt{2k_BT}}$	2 (**.6**)
$(\Gamma^{(i)})^{-1}$	$\frac{\gamma}{\gamma_m^i}$	10
$u^{(i)}$	$\frac{\kappa^{(i)}}{F_d^i}\sqrt{\frac{2k_BT}{\bar{\kappa}}}$	.9 (**.7**)
$\tilde{a}^{(i)}$	$\frac{a^{(i)}\gamma}{\bar{\kappa}}$	$1.5\times\ 10^{-4}$ $(\mathbf{6.0\times\ 10^{-5}})$
$\tilde{d}^{(i)}$	$\frac{d^{(i)}\gamma}{\bar{\kappa}}$	$1.9\times\ 10^{-5}, (\mathbf{8.1\times\ 10^{-5}})$

and variance

$$\frac{1}{2\sum_{j=1}^N b^{(j)}\tilde{\kappa}^{(j)}}+\frac{1}{2\tilde{\kappa}^{(i)}}$$

3.3 Homogenization for a two motor system.

We now will focus on dynamics for a two motor system during a processive run. At any one time, either one or two motors may be attached to the microtubule, which gives three possible states, each with their own SDEs describing motion (as discussed in Section 2.1, we do not consider a fully detached system). For the following analysis, we will make use of the assumption that the attachment and detachment rates are slow relative to the attached motor dynamics ($\tilde{a},\tilde{d}\ll\epsilon$), so that when two motors are attached, their configuration reaches a statistical equilibrium before one of the motor detaches.

One challenge in characterizing the progress of the motor-cargo system through phases of attachment and detachment is the choice of a "tracking" variable that remains well-defined in the various states of motor attachment. The cargo variable $\tilde{Z}(\tilde{t})$ is an obvious candidate since in experiments it is the largest and most easily observed object, and whose progress of space is of practical importance. Mathematically, though, as shown in the dimensional analysis from Subsection 3.1, the cargo will tend to fluctuate more rapidly than attached motors, which makes it somewhat awkward to use as a tracking variable on long time scales. We therefore introduce the variable $\tilde{M}(\tilde{t})$ for the mean cargo position at time $\tilde{t}$ under the quasi-stationary distribution $p_{\tilde{Z}|\tilde{\mathbf{X}}^{(a)},\mathbf{B}}$ (15) for the cargo given the current positions of the motors attached to the microtubule at time $\tilde{t}$:

$$\tilde{M}(\tilde{t})\equiv\int_{-\infty}^{\infty}\tilde{z}p_{\tilde{Z}|\tilde{\mathbf{X}}^{(a)},\mathbf{S}}(\tilde{z}|\mathbf{X}(\tilde{t}),\mathbf{B}(\tilde{t}))=\left[\frac{\sum_{j=1}^N B^{(j)}(\tilde{t})\tilde{\kappa}^{(j)}\tilde{X}^{(j)}(\tilde{t})}{\sum_{j=1}^N B^{(j)}(\tilde{t})\tilde{\kappa}^{(j)}}-\frac{\tilde{F}}{\sum_{j=1}^N B^{(j)}(\tilde{t})\tilde{\kappa}^{(j)}}\right] \tag{25}$$

One can check that $\tilde{M}(\tilde{t})$ is equivalent to the deterministic mechanical equilibrium of the cargo, for given attached motor positions, in the absence of stochastic fluctuations. Markov chain models for cargo transport with attaching and detaching motors often model the cargo as always being exactly at this position $\tilde{M}(\tilde{t})$ of force balance relative to the attached motors; our present model accounts for cargo fluctuations about this mechanical equilibrium. Nonetheless, $\tilde{M}$ is a more convenient variable for tracking the progress of the cargo through episodes of attachment and detachment. Moreover, the cargo position $\tilde{Z}(\tilde{t})$, under our time scale separation assumptions, has a Gaussian distribution centered at $\tilde{M}(\tilde{t})$ with standard deviation no larger than $\max_{1\le j\le N}\{\frac{1}{2\tilde{\kappa}^{(j)}}\}$ (see Eq. (15)). Consequently, the long-time statistical transport properties of the cargo position $\tilde{Z}(\tilde{t})$ and the tracking variable $\tilde{M}(\tilde{t})$ are equivalent.

The simplest case to analyze is when exactly one of the two motors is attached. For the discussion of this case, we will take i to be the index of the motor which is attached, and $i' = 3 - i$ as the index of the detached motor. Then from Eq. (25),

$$\tilde{M}(\tilde{t}) = \tilde{X}^{(i)}(\tilde{t}) - \tilde{F}/\tilde{\kappa}^{(i)}. \tag{26}$$

We may then use equations (19) and (26) to obtain an averaged approximation

$$M(\bar{t}) = \bar{X}^{(i)}(\bar{t}) - \tilde{F}/\tilde{\kappa}^{(i)} \tag{27}$$

for $\tilde{M}(\bar{t}/\epsilon)$, satisfying

$$dM(\bar{t}) = \bar{V}_i d\bar{t} + \sqrt{\rho^{(i)}} dW^{(i)}(\bar{t}). \tag{28}$$

Equation (20) is then a constant drift

$$\bar{V}_i = \sqrt{\frac{\tilde{\kappa}^{(i)}}{\pi}} \frac{\epsilon^{(i)}}{\bar{\epsilon}} \int_{\mathbb{R}} g(s^{(i)} y) \exp(-\tilde{\kappa}^{(i)}(y - \tilde{F}/\tilde{\kappa}^{(i)})^2) dy. \tag{29}$$

We can also obtain effective velocity and diffusivity for when both motors are attached. For known motor positions $x^{(1)}, x^{(2)}$, we can express the cargo-averaged drift coefficients purely in terms of the signed displacement $r = x^{(1)} - x^{(2)}$ between the motors:

$$\bar{V}_1^{(1,2)}(x^{(1)}, x^{(2)}) = G^{(1)}(x^{(1)} - x^{(2)}), \tag{30}$$

$$\bar{V}_2^{(1,2)}(x^{(1)}, x^{(2)}) = G^{(2)}(x^{(1)} - x^{(2)}), \tag{31}$$

$$G^{(i)}(r) = \frac{\epsilon^{(i)}}{\bar{\epsilon}} \sqrt{\frac{2}{\pi}} \int_{\mathbb{R}} g(s^{(i)} y) \exp\left(-2 \left(y + \frac{(-1)^i \tilde{\kappa}^{(i')} r}{2} - \frac{\tilde{F}}{2} \right)^2 \right) dy. \tag{32}$$

This representation is achieved by the change of variable $y = x^{(i)} - z$ in (20). Note that when describing effective drift, diffusion, and/or detachment rates from various states of attachment, we will typically list the indices of the attached motors in the subscript (without parentheses or brackets), and when needed, indicating by a parenthesized superscript the index of which motor in

that state is being described by the parameter. Further simplifying notation, let

$$G_+(r) = \frac{\tilde{\kappa}^{(1)}}{2} G^{(1)}(r) + \frac{\tilde{\kappa}^{(2)}}{2} G^{(2)}(r), \tag{33}$$

$$G_-(r) = G^{(1)}(r) - G^{(2)}(r). \tag{34}$$

The tracking variable (25) in this state is, from Eq. (17),

$$\tilde{M}(\tilde{t}) = (\tilde{\kappa}^{(1)} \tilde{X}^{(1)}(\tilde{t}) + \tilde{\kappa}^{(2)} \tilde{X}^{(2)}(\tilde{t}) - \tilde{F})/2, \tag{35}$$

Passing now to the long time scale $\bar{t}/\epsilon$, we can recast the cargo-averaged dynamics (19) for the attached motors in terms of the tracking variable

$$M(\bar{t}) = (\tilde{\kappa}^{(1)} \bar{X}^{(1)}(\bar{t}) + \tilde{\kappa}^{(2)} \bar{X}^{(2)}(\bar{t}) - \tilde{F})/2 \tag{36}$$

and the (signed) intermotor displacement

$$R(\bar{t}) = \bar{X}^{(1)}(\bar{t}) - \bar{X}^{(2)}(\bar{t}), \tag{37}$$

which gives

$$dM(\bar{t}) = G_+(R(\bar{t}))d\bar{t} + \frac{\sqrt{\rho^{(1)}(\tilde{\kappa}^{(1)})^2}}{2} dW^{(1)}(\bar{t}) + \frac{\sqrt{\rho^{(2)}(\tilde{\kappa}^{(2)})^2}}{2} dW^{(2)}(\bar{t}) \tag{38}$$

$$dR(\bar{t}) = G_-(R(\bar{t}))dt + \sqrt{\rho^{(1)}} dW^{(1)}(\bar{t}) - \sqrt{\rho^{(2)}} dW^{(2)}(\bar{t}). \tag{39}$$

Under the regime where switching is slow relative to detachment, we may perform averaging on the internal variable R in order to obtain the effective velocity and diffusion for M. As (39) does not depend on M, the stationary distribution for the process R is a potential function

$$p_R(r) = C_R \exp\left[\frac{2}{\rho^{(1)} + \rho^{(2)}} \int_0^r G_-(r')dr'\right], \quad -\infty < r < \infty, \tag{40}$$

where C_R is a normalizing constant. Thus, the effective velocity is

$$\bar{V}_{1,2} = \int_{\mathbb{R}} G_+(r) p_R(r) dr. \tag{41}$$

The computation for effective diffusivity is more complicated. In [23] a central limit theorem for stationary stochastic differential equations from [43] was employed to this end for the case of identical motors. That theorem assumes the stochastic driving terms in the SDE system to be uncorrelated, which in general does not occur for nonidentical motors in (38)-(39). Fortunately, only minor modifications are needed to generalize the derivation for effective diffusion found in [39] for the case of uncorrelated stochastic driving. Under this approach, we arrive at the effective diffusion

$$D^{(1,2)} = \int_{-\infty}^{\infty} \left(\frac{2}{\rho^{(1)} + \rho^{(2)}}\right) \left(\int_{-\infty}^{r} (G_+(m) - \bar{V}_{1,2}) p_R(m) dm\right)^2 \frac{1}{p_R(r)} dr$$
$$+ \left(\frac{\rho^{(1)}\tilde{\kappa}^{(1)} - \rho^{(2)}\tilde{\kappa}^{(2)}}{\rho^{(1)} + \rho^{(2)}}\right) \int_{\mathbb{R}} (G_+(r) - \bar{V}_{1,2}) p_R(r) \cdot r dr + \frac{\rho^{(1)}(\tilde{\kappa}^{(1)})^2 + \rho^{(2)}(\tilde{\kappa}^{(2)})^2}{8}.$$

A one dimensional approximation of the cargo-tracking variable on long time scales $M(\bar{t}) \approx \tilde{M}(\bar{t}/\epsilon)$can now be given by

$$dM(\bar{t}) = \bar{V}_{1,2}d\bar{t} + \sqrt{2D_{1,2}}dW(\bar{t}), \tag{42}$$

where $W(\bar{t})$ is a standard Brownian motion. A full derivation of the effective diffusion can be found in Appendix C.

4 Effective statistics for the slow switching regime.

4.1 Effective detachment rates

In keeping with the tracking variable coordinate system for two motors presented in Section 3.3, we express detachment rates $\bar{d}^{(i)}(\mathbf{x}, \mathbf{s})$ in (21) under the $\bar{t}$ time scale solely through intermotor distance $r = x^{(1)} - x^{(2)}$, where we write $\bar{d}^{(i)}((x^{(1)}, x^{(2)}), (1, 1)) = \bar{d}^{(i)}_{1,2}(x^{(1)} - x^{(2)})$. This is done through a substitution $y = x^{(i)} - z$, resulting in

$$\bar{d}^{(i)}_{1,2}(r) = \sqrt{\frac{2}{\pi}}\frac{\tilde{d}^{(i)}_0}{\bar{\epsilon}} \int_{\mathbb{R}} \Upsilon\left(u^{(i)}y\right) \exp\left(-2\left(y - \frac{1}{2}((-1)^{i+1}\tilde{\kappa}^{(i')}r - \tilde{F})\right)^2\right) dy. \tag{43}$$

From our assumptions about the detachment time scale being slower than the attached motor time scale ($\tilde{d}^{(i)} \ll \epsilon^{(i)}$) in Section **??**, we can apply stochastic averaging (CITE) to approximate $\bar{d}^{(i)}_{1,2}(r)$ by averaging over the stationary distribution $p_R(r)$ for the motor separation R, which gives the constant effective detachment rates of

$$\bar{d}^{*(i)}_{1,2} = \int_{\mathbb{R}} \bar{d}^{(i)}_{1,2}(r)p_R(r)dr. \tag{44}$$

An effective total rate of detachment from the state of both motors attached is then

$$\bar{d}^{*}_{1,2} = \bar{d}^{*(1)}_{1,2} + \bar{d}^{*(2)}_{1,2}. \tag{45}$$

In the case of a single attached motor with index i, we have a constant attachment rate $\tilde{a}^{(i')}$, and detachment rate $\tilde{d}^{(i)}(x^{(i)}, z)$ that is dependent on the attached motor position $x^{(i)}$ and cargo position z. On the longer $\bar{t} = \bar{\epsilon}\tilde{t}$ time scale, the slow switching approximation would reduce the detachment rate (21) to a constant:

$$\bar{d}^{*}_{i} = \sqrt{\frac{\tilde{\kappa}^{(i)}}{\pi}}\frac{\tilde{d}^{(i)}_0}{\bar{\epsilon}} \int_{\mathbb{R}} \Upsilon(u^{(i)}y) \exp(-\tilde{\kappa}^{(i)}(y - \tilde{F}/\tilde{\kappa}^{(i)})^2)dy. \tag{46}$$

and simply rescale the constant attachment rates:

$$\bar{a}^{*(i)} \equiv \frac{\tilde{a}^{(i)}}{\bar{\epsilon}}. \tag{47}$$

4.2 Jumps at switching events

When a motor detaches from a state of two attached motors, there is an immediate change in the force balance between motors and cargo. The cargo, which is fast relative to a single bound motor, quickly adjusts to the new motor configuration. This results in a jump of the tracking variable position. A similar readjustment occurs with motor attachment. See Fig. 4 in Section 6 for simulations depicting jumps in cargo positions. In this subsection, we describe distributions of jump sizes at these switching events. This is done under the assumption of slow switching, so that we may assume the intermotor distance variable $R(t)$ in the state of two attached motors has achieved its stationary distribution.

4.2.1 Jumps at detachment from state of both motors attached

We focus in this subsection on the statistical behavior of the system at a random time $\tau_{\rm d}$ at which one of the two motors detaches ($\mathbf{B}(\tau_{\rm d}^-) = (1,1) \neq \mathbf{B}(\tau_{\rm d})$). The distribution of $R(\tau_{\rm d}^-)$ just before detachment will not be the same as the stationary distribution of $R(t)$ due to the dependence of the detachment rate on $R(t)$. Rather, the distribution of the intermotor distance just before first detachment $R^{(\rm d)} = R(\tau_{\rm d}^-)$ will be reweighted by the detachment rate, yielding the probability density:

$$p_{R^{(\rm d)}}(r) = \frac{(\bar{d}_{1,2}^{(1)}(r) + \bar{d}_{1,2}^{(2)}(r))p_R(r)}{\bar{d}_{1,2}^*} \tag{48}$$

This can be readily argued by considering a short time interval of length Δt over which fluctuations in $R(t)$ are negligible, using Bayes' rule to calculate the conditional probability of $R(t)$ given that detachment occurs during the time interval, and passing to the limit $\Delta t \downarrow 0$.

Next, we denote by $J^{(d)}$ the index of the motor which first detaches from the two-motor-attached state (at the random time $\tau_{\rm d}$). From the standard theory of continuous-time Markov chains,

$$\mathbb{P}(J^{(d)} = i | R(\tau_{\rm d}) = r) = \frac{\bar{d}_{1,2}^{(i)}(r)}{\bar{d}_{1,2}^{(1)}(r) + \bar{d}_{1,2}^{(2)}(r)}$$

and thus the unconditional probability that motor i detaches first is:

$$p_d^{(i)} \equiv \mathbb{P}(J^{(d)} = i) = \int_{-\infty}^{\infty} \frac{\bar{d}_{1,2}^{(i)}(r)}{\bar{d}_{1,2}^{(1)}(r) + \bar{d}_{1,2}^{(2)}(r)} p_{R^{(\rm d)}}(r) dr = \frac{\bar{d}_{1,2}^{*(i)}}{\bar{d}_{1,2}^*}.$$

This is consistent with the coarse-grained description of the attachment states of the motors, under the slow switching approximation, still having the properties of a continuous-time Markov chain.

The jump of the tracking variable M at detachment is essentially a result of how the mean position of cargo relies upon the number of attached motors.

This is represented by the difference between equations (27) and (36). Consider, for now, that motor 2 detaches ($J^{(d)} = 2$) from the two-motor-attached state at time $\tau_{\rm d}$ The jump size $\Delta M_2^{(\rm d)} = M(\tau_{\rm d}) - M(\tau_{\rm d}^-)$ will be

$$\begin{aligned}\Delta M_2^{(\rm d)} &= \left[\bar{X}^{(1)}(\tau_{\rm d}^-) - \frac{\tilde{F}}{\tilde{\kappa}^{(1)}}\right] - \frac{1}{2}\left[\tilde{\kappa}^{(1)}\bar{X}^{(1)}(\tau_{\rm d}^-) + \tilde{\kappa}^{(2)}\bar{X}^{(2)}(\tau_{\rm d}^-) - \tilde{F}\right] \\ &= \frac{\tilde{\kappa}^{(2)}}{2}R(\tau_{\rm d}^-) - \frac{\tilde{\kappa}^{(2)}\tilde{F}}{2\tilde{\kappa}^{(1)}}\end{aligned}$$

and thus have the distribution

$$\Delta M_2^{(\rm d)} \sim \frac{\tilde{\kappa}^{(2)}}{2}\left(R^{(\rm d)} - \frac{\tilde{F}}{\tilde{\kappa}^{(1)}}\right).$$

A similar calculation shows that when motor 1 detaches ($J^{(d)} = 1$), then $\Delta M_1^{(\rm d)} \sim \frac{\tilde{\kappa}^{(1)}}{2}(-R^{(\rm d)} - \frac{\tilde{F}}{\tilde{\kappa}^{(2)}})$. In more compact form, the jump in the tracking variable when motor i detaches from the two-motor-attached state has distribution:

$$\Delta M_i^{(\rm d)} \sim \frac{\tilde{\kappa}^{(i)}}{2}\left((-1)^i R^{(\rm d)} - \frac{\tilde{F}}{\tilde{\kappa}^{(i')}}\right). \tag{49}$$

where $R^{(\rm d)}$ has probability density function given in Eq. (48).

4.2.2 Jumps at attachment of second motor from state of one motor attached

We now compute the statistics of the jumping distances at a time $\tau_{\rm a}$ before which only one motor is attached, and at which time the second motor (with index $J^{(a)}$) attaches. Suppose first that we begin with motor 1 attached, then motor 2 attaches ($J^{(a)} = 2$) at time $\tau_{\rm a}$.

From Eq. (22), detached motor 2 has a location distributed, conditional on the position of attached motor 1, as

$$\bar{X}^{(2)}(\tau_{\rm a}^-) \sim N(\bar{X}^{(1)}(\tau_{\rm a}^-) - \tilde{F}/\tilde{\kappa}^{(1)}, 1/(\tilde{\kappa}^{(1)}\tilde{\kappa}^{(2)})), \tag{50}$$

where $N(\mu, \sigma^2)$ denotes a normally distributed random variable with mean μ and variance σ^2. Under our model that the attaching motors attaches at a position governed by its detached spatial distribution, the jump in the central coordinate upon attachment of motor 2 is then

$$\Delta M_2^{(\rm a)} = \frac{1}{2}\left[\tilde{\kappa}^{(1)}\bar{X}^{(1)}(\tau_{\rm a}^-) + \tilde{\kappa}^{(2)}\bar{X}^{(2)}(\tau_{\rm a}^-) - \tilde{F}\right] - \left[\bar{X}^{(1)}(\tau_{\rm a}^-) - \frac{\tilde{F}}{\tilde{\kappa}^{(1)}}\right] \tag{51}$$

$$\sim N\left(0, \frac{\tilde{\kappa}^{(2)}}{4\tilde{\kappa}^{(1)}}\right). \tag{52}$$

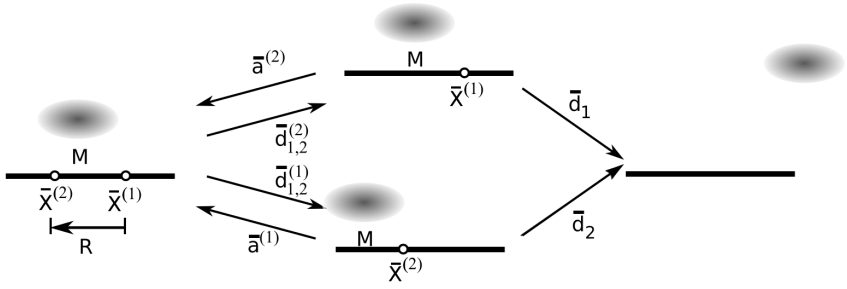

Fig. 2: **Switched diffusion model.** Left: A cargo with two attached motors with cargo tracking variable M evolving according to (42). Each motor i can detach with rate $\bar{d}^{(i)}_{1,2}(R)$ (43) depending on the displacement R between the attached motors. Middle: The cargo tracking variable M with one attached motor evolves according to a constant coefficient stochastic differential equation (28). From these states, the system either detaches completely (as shown in the rightmost part of the figure), with effective rate given in (**??**) or returns to having two attached motors, with rates $\tilde{a}_i$.

.

More generally, when motor i is the detached motor which attaches, the tracking coordinate jumps by an amount

$$\Delta M_i^{(\mathrm{a})} \sim N\left(0, \frac{\tilde{\kappa}^{(i)}}{4\tilde{\kappa}^{(i')}}\right), \tag{53}$$

which is always mean zero even when the motors are nonidentical.

4.3 Coarse-Grained Markov Chain Model

Under our asymptotic approximations including the slow switching approximation, our original model based on stochastic differential equations with configuration-dependent detachment rates for the motors has been coarse-grained into simple continuous-time Markov chain dynamics on the state space of attachment states, together with a tracking variable $M(t)$ which may be thought of as an accumulated reward function associated with the Markov chain. We will label these attachment states by a list ϖ of the indices of the attached motors, as indicated in Figure 3, and properties of the cargo transport in an attachment state with the attached state list in parentheses in the superscript. The transition rates between states are now all constant, also indicated in Figure 3.

The state $\varpi = \emptyset$ acts as an absorbing state terminating the processive run. In each the other three states, the tracking variable undergoes a constant-

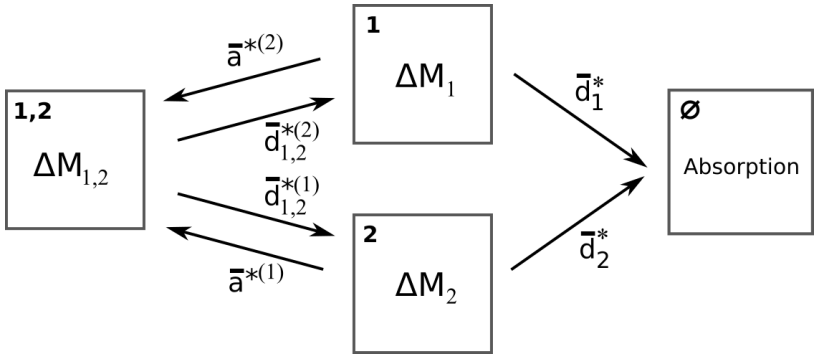

Fig. 3: **Coarse-grained Markov chain model.** Under the assumption of slow switching, the switched diffusion model (see Fig. 2) is further coarsened by averaging intermotor distance. The random displacement ΔM_ϖ for each attachment state ϖ (shown in the upper left corner of each box) is then found through (54), for which we find explicit statistics in Section 5. Detachment rates $\bar{d}^{*(i)}_{1,2}$ from the state of two attached motors, given by (44), are now constants coarse-grained with respect to intermotor distance.

coefficient drift-diffusion dynamics, with the formulas for the effective coefficients presented in Subsection 3.3. Thus, a visit to a state $\varpi \neq \emptyset$ is associated to a tracking variable increment

$$\Delta M_\varpi = V_\varpi \Delta T_\varpi + \sqrt{2D_\varpi}\Delta W(\Delta T_\varpi), \tag{54}$$

where T_ϖ is the duration of the visit to state ϖ, and $\Delta W(t) \sim N(0,t)$ denotes the increment of the Wiener process over a time t. Moreover, as we noted in Section 4.2, transitions between attachment states are also associated with jumps in the tracking variable. Namely, when a motor i detaches from the two-motor-attached state (transition $(1,2) \to (i')$), the tracking variable undergoes a jump $\Delta M_i^{(\mathrm{d})}$ given by equation (49). When a motor i attaches to form the two-motor-attached state (transition $(i') \to (1,2)$), the tracking variable undergoes a jump $\Delta M_i^{(\mathrm{a})}$, given by equation (53). A technical presentation of the joint dynamics of the Markov chain and tracking variable can be found in Appendix A.

5 Effective Transport Characterization

For a cooperative system of two motors, we have provided in the previous section a coarse-grained approximation of the stochastic process governed by equations (11)-(13). Appendix A for the process in time change representation form). These simplified equations are adequate, under the conditions of validity of the asymptotic approximations, for computing effective transport properties of the motor-cargo complex. We begin in Subsection **??** by computing the

processivity measures: the mean and variance of the run time and run length. Then we turn in Subsection 5.2 to the theoretical calculation of the effective velocity and diffusivity of the motor-cargo complex. The proper definition of these transport statistics is not entirely obvious for a motor-cargo complex that eventually detaches and terminates progress along the microtubule. We discuss two distinct mathematical framings of velocity and diffusivity in this context, and relate them to approaches used in analyses of previous models as well as to experimental approaches. We then, in turn, compute the velocity and diffusivity under each of the two mathematical interpretations.

5.1 Processivity

The slow switching dynamics can be viewed as a 4-state Markov chain labeled by attachment state $\{(1,2),(1),(2),\emptyset\}$, denoting full attachment, motor 1 or 2 attached, and complete detachment, respectively. Starting from the fully attached state $(1,2)$, the motor-cargo complex will undergo a random number N_{c} of *full cycles* between 2-motor and 1-motor attached states (either $(1,2) \to (1) \to (1,2)$ or $(1,2) \to (2) \to (1,2)$) and ultimately a *terminal cycle* (either $(1,2) \to (1) \to \emptyset$ or $(1,2) \to (2) \to \emptyset$) ending in complete detachment. Thus N_{c} is a geometric random variable with mean $\frac{p}{1-p}$, where the probability of complete detachment is

$$p = p_d^{(2)} \frac{\bar{d}_1^*}{\bar{a}^{*(2)} + \bar{d}_1^*} + (1 - p_d^{(2)}) \frac{\bar{d}_2^*}{\bar{a}^{*(1)} + \bar{d}_2^*}. \tag{55}$$

For each cycle (either complete or terminal), time advances by a random increment

$$\Delta T_{\mathrm{c}} = \Delta T_{1,2} + \Delta T_{J^{(d)\prime}}, \tag{56}$$

The distributions of time $\Delta T_{1,2}$ spent in the fully attached and time ΔT_i spent in the state with only motor i attached are exponentially distributed random variables with the indicated means:

$$\Delta T_{1,2} \sim \mathrm{Exp}((\bar{d}_{1,2}^*)^{-1}), \quad \Delta T_i \sim \mathrm{Exp}((\bar{a}^{*(i')} + \bar{d}_{1,2}^{*(i)})^{-1}). \tag{57}$$

Note that, because of the independence of the residence time in a state and the next state in a continuous time Markov chain (CITE Lawler), the distribution of ΔT_i is unaffected by the implicit conditioning on the Markov chain returning to the fully attached state from the partially attached state.

Similarly, in each cycle the tracking variable will advance by a random increment

$$\Delta M_{\mathrm{c}} = \Delta M_{1,2} + \Delta M_{J^{(d)\prime}} + \overline{\Delta M}^{(\mathrm{a})}_{J^{(d)}} + \Delta M^{(\mathrm{d})}_{J^{(d)}}. \tag{58}$$

Here, we write $\overline{\Delta M}_i^{(\mathrm{a})}$ to extend the the state space of $\Delta M_i^{(\mathrm{a})}$ to include the possibility of complete detachment, in which case no attachment occurs and

thus $\overline{\Delta M}_i^{(\mathrm{a})} = 0$. The distributions for $\Delta M_i^{(\mathrm{d})}$ and $\Delta M_i^{(\mathrm{a})}$ given in (49) and (53) are independent of the time spent in any given Markov chain state. On the other hand, from (28) and (42),

$$\Delta M_{1,2}|\Delta T_{1,2} \sim N(\bar{V}_{1,2}\Delta T_{1,2}, 2D_{1,2}\Delta T_{1,2}), \tag{59}$$

$$\Delta M_i|\Delta T_i \sim N(\bar{V}_i\Delta T_i, \rho^{(i)}\Delta T_{1,2}). \tag{60}$$

Like the distributions for $\Delta T_{1,2}$ and ΔT_i, run lengths are independent on whether the motor system eventually returns to a two motor attached state.

We now compute statistics for run lengths and times for different attachment states involved in a cycle. For evolution with two attached motors, we invoke the law of total expectation to obtain

$$\mathbb{E}[\Delta M_{1,2}] = \frac{\bar{V}_{1,2}}{\bar{d}^*_{1,2}}. \tag{61}$$

From (59), we may use the law of total variance, conditioning on $\Delta T_{1,2}$, to obtain

$$\mathrm{Var}(\Delta M_{1,2}) = \frac{2D_{1,2}}{\bar{d}^*_{1,2}} + \left(\frac{\bar{V}_{1,2}}{\bar{d}^*_{1,2}}\right)^2 \tag{62}$$

From (49), (53), and (54) we can easily compute the following statistics

$$\mathbb{E}(\Delta M_i) = \frac{\bar{V}_i}{\bar{a}^{*(i')} + \bar{d}^*_i}, \qquad \mathrm{Var}(\Delta M_i) = \frac{2D_i}{\bar{a}^{*(i')} + \bar{d}^*_i} + \left(\frac{\bar{V}_i}{\bar{a}^{*(i')} + \bar{d}^*_i}\right)^2,$$

$$\mathbb{E}(\Delta M_i^{(\mathrm{a})}) = 0, \qquad \mathrm{Var}(\Delta M_i^{(\mathrm{a})}) = \frac{1}{4}\frac{\tilde{\kappa}^{(i)}}{\tilde{\kappa}^{(i')}}, \tag{63}$$

$$\mathbb{E}(\Delta M_i^{(\mathrm{d})}) = \frac{\tilde{\kappa}^{(i)}}{2}\left((-1)^i\mu_{R^{(\mathrm{d})}} - \frac{\tilde{F}}{\tilde{\kappa}^{(i')}}\right), \quad \mathrm{Var}(\Delta M_i^{(\mathrm{d})}) = \frac{1}{4}(\tilde{\kappa}^{(i)})^2\sigma^2_{R^{(\mathrm{d})}}. \tag{64}$$

Here, we note that $\mu_{R^{(\mathrm{d})}}$ and $\sigma^2_{R^{(\mathrm{d})}}$ may be computed directly from the density given in (48) . For the special case of constant detachment rates, $\mu_{R^{(\mathrm{d})}} = \mu_R$. We also note that the random variables of run time and length are independent of whether an ensemble is in a complete or terminal cycle. However, this is not the case for the random index $J^{(d)}$, which we will discuss in Section 5.2.1.

We now consider the total run time T and total run length $M(T)$ taken by an ensemble of a cargo with two cooperative motors before complete detachment. For simplicity, we take the system to start with both motors are attached. Then T is just the first passage time of the coarse-grained Markov chain from state $(1,2)$ to the state $\emptyset$, and $M(T)$ is the increment in the cargo tracking variable M until absorption at the fully detached state $\emptyset$. We may then write T and $M(T)$ as random sums of iid random variables ΔT_{c}^j and ΔM_{c}^j, $j \geq 1$, where the random index $N_{\mathrm{c}} + 1$ is a stopping time of ΔT_{c}^j:

$$T = \sum_{j=1}^{N_{\mathrm{c}}+1} \Delta T_{\mathrm{c}}^j, \quad M(T) = \sum_{j=1}^{N_{\mathrm{c}}+1} \Delta M_{\mathrm{c}}^j. \tag{65}$$

We may use Wald's identity (see Th. 14.6 of [44]) to obtain

$$\mathbb{E}[T] = \mathbb{E}[N_c + 1]\mathbb{E}[\Delta T_c], \tag{66}$$
$$\mathbb{E}[M(T)] = \mathbb{E}[N_c + 1]\mathbb{E}[\Delta M_c]. \tag{67}$$

Variances and covariance may also be calculated from the second Wald identity (see Th. 2.4.5 of [45]) as

$$\begin{aligned}
\mathrm{Var}(T) &= \mathbb{E}[N_c + 1]\,\mathrm{Var}(\Delta T_c) + \mathbb{E}^2[\Delta T_c]\,\mathrm{Var}(N_c + 1), \\
\mathrm{Var}(M(T)) &= \mathbb{E}[N_c + 1]\,\mathrm{Var}(\Delta M_c) + \mathbb{E}^2[\Delta M_c]\,\mathrm{Var}(N_c + 1), \\
\mathrm{Cov}(T, M(T)) &= \mathbb{E}[N_c + 1]\mathrm{Cov}(\Delta T_c, \Delta M_c) + \mathbb{E}[\Delta T_c]\mathbb{E}[\Delta M_c]\,\mathrm{Var}(N_c + 1).
\end{aligned} \tag{68}$$

Explicit expressions for the cycle statistics in (66)-(68) will be provided in the Section 5.2.2.

5.2 Effective velocity and diffusion

The characterization of the effective velocity and diffusivity is not so straightforward for a motor-cargo complex that eventually detaches from a microtubule. One cannot directly take the long-time limit of the ratio of distance traveled to time, since the motor-cargo complex will detach at a finite time. Of course, for cooperative motor models that explicitly model a rate for reattachment for the motors even from the fully detached state, one can of course define an effective velocity and diffusivity in the usual way, essentially averaging progress over both phases where the motor-cargo complex is attached or detached from a microtubule [**?**] (CITE parattachlong). While such an effective velocity is meaningful for characterizing transport, it does not relate so naturally to experimental observations of particular cargo, which are tracked only while they appear to be attached to a microtubule.

In order to describe correspondingly the effective velocity diffusivity of cargo during periods where at least one of its motors is attached to a microtubule, two distinct definitions of effective velocity and diffusivity suggest themselves:

1. Considering a single experiment with a long run length and run time, forming the ratio $\frac{M(t)}{t}$ at times t before detachment, and defining the long-run velocity V_{run} as the idealized $t \to \infty$ limit. The long-run diffusivity would be computed similarly from the long-time limit of the ratio $\frac{(M(t)-V_{\mathrm{run}}t)^2}{2t}$, conditioned on the complex not detaching before time t. Let ΔM_f and ΔT_f denote, respectively, the cycle run length and run time under the condition $\mathcal{A}$ that the cycle ends with a return to the two-motor-attached state ($(1,2) \to (i) \to (1,2)$) rather than to the detachment of the complex ($(1,2) \to (i) \to \emptyset$). Expressing $M(t)$ as a sum over attachment/detachment cycles as in (REF) and applying the renewal-reward theorem [46] allows the long-run velocity and diffusivity to be expressed in terms of ΔM_f and

ΔT_{f}:

$$V_{\mathrm{run}} = \frac{\mu_{\Delta M_{\mathrm{f}}}}{\mu_{\Delta T_{\mathrm{f}}}}, \tag{69}$$

$$D_{\mathrm{run}} = \frac{1}{2}\left(\frac{\mu_{\Delta M_{\mathrm{f}}}\sigma^2_{\Delta T_{\mathrm{f}}}}{\mu^3_{\Delta T_{\mathrm{f}}}} + \frac{\sigma^2_{\Delta M_{\mathrm{f}}}}{\mu_{\Delta T_{\mathrm{f}}}} - \frac{2\mu_Z\sigma_{\Delta M_{\mathrm{f}},\Delta T_{\mathrm{f}}}}{\mu^2_{\Delta T_{\mathrm{f}}}}\right) \tag{70}$$

$$= \frac{V^2_{\mathrm{run}}\sigma^2_{\Delta T_{\mathrm{f}}} + \sigma^2_{\Delta M_{\mathrm{f}}} - 2V_{\mathrm{run}}\sigma_{\Delta M_{\mathrm{f}},\Delta T_{\mathrm{f}}}}{2\mu_{\Delta T_{\mathrm{f}}}}, \tag{71}$$

As shown in [47], the renewal-reward formulas (74)-(71) still apply if the long time t occurs in the middle of a cycle.

2. Pooling run times T^j and run lengths $M(T^j)$ over independent experiments $j = 1, \ldots, S$, and defining the ensemble velocity and diffusivity as:

$$V_{\mathrm{pool}} \equiv \lim_{S\to\infty} \frac{\sum_{j=1}^{S} M(T^j)}{\sum_{j=1}^{S} T^j}, \tag{72}$$

$$D_{\mathrm{pool}} \equiv \lim_{S\to\infty} \frac{\left(\sum_{j=1}^{S}(M(T^j) - V_{\mathrm{pool}}T^j)\right)^2}{2\sum_{j=1}^{S} T^j}. \tag{73}$$

By the law of large numbers, these quantities can be expressed in terms of statistical averages:

$$V_{\mathrm{pool}} = \frac{\mu_{M(T)}}{\mu_T} = \frac{\mu_{\Delta M_{\mathrm{c}}}}{\mu_{\Delta T_{\mathrm{c}}}}, \tag{74}$$

$$D_{\mathrm{pool}} = \frac{V^2_{\mathrm{pool}}\sigma^2_T + \sigma^2_{M(T)} - 2V_{\mathrm{pool}}\sigma_{M(T),T}}{2\mu_T}. \tag{75}$$

The ensemble definition ostensibly matches with how velocity and diffusivity are typically computed in experiments, but we must bear in mind that experiments typically only measure runs of a cargo that are sufficiently long, since short runs are difficult to detect or disambiguate from noise. Thus, the actual experimental values might fall somewhere between the ensemble and long-run definitions given above, so we will study both. Stochastic simulations typically also compute velocity (and sometimes diffusivity) using the ensemble definitions given above, though some simulation studies compute velocities and diffusivities in each run, and then average the single-run velocities and diffusivities over the ensemble. The latter has no inherent connection to long-time properties, but would be approximated by the long-run definitions if the run times happened to be sufficiently long in some statistical sense.

5.2.1 Long-Run Velocity and Diffusivity

In the calculation of velocity and diffusivity for an idealized single long run, we condition on at least one motor remaining connected to the microtubule at all times. This leads to modifying the statistical calculation in terms of

the cycles by conditioning on the event $\mathcal{A}$ that the cycle ends in a state of two attached motors, rather than complete detachment of all motors. By the above-mentioned independence of residence time of a state and the next state, this attachment assumption does not affect distributions of attachment and detachment times given in (57), nor the components of the cargo-tracking displacements $\Delta M_{1,2}$, ΔM_i, $\Delta M_i^{(\mathrm{a})}$, and $\Delta M_i^{(\mathrm{d})}$.

Let $J_{\mathrm{c}}^{(d)}$ denote the random index of detachment $J^{(d)}$ conditioned on the event of a complete cycle, which we denote $\mathcal{A}$. We can compute the distribution of $J_{\mathrm{c}}^{(d)}$ through Bayes' rule, with

$$p_{d|\mathcal{A}}^{(i)} := \mathbb{P}(J_{\mathrm{c}}^{(d)} = i) = \mathbb{P}(J^{(d)} = i|\mathcal{A}) \tag{76}$$

$$= \mathbb{P}(\mathcal{A}|J^{(d)} = i)\frac{\mathbb{P}(J^{(d)} = i)}{\mathbb{P}(\mathcal{A})} = \frac{\frac{\bar{a}^{(i)}}{\bar{d}^*_{i'}+\bar{a}^{(i)}}\left(\frac{\bar{d}^{*(i)}_{1,2}}{\bar{d}^*_{1,2}}\right)}{\frac{\bar{a}^{(i)}}{\bar{d}^*_{i'}+\bar{a}^{(i)}}\left(\frac{\bar{d}^{*(i)}_{1,2}}{\bar{d}^*_{1,2}}\right) + \frac{\bar{a}^{(i')}}{\bar{d}^*_{i}+\bar{a}^{(i')}}\left(\frac{\bar{d}^{*(i')}_{1,2}}{\bar{d}^*_{1,2}}\right)}. \tag{77}$$

We can then express the run length and time of a complete cycle as

$$\Delta T_{\mathrm{f}} = \Delta T_{1,2} + \Delta T_{J_{\mathrm{f}}^{(d)},}, \tag{78}$$

$$\Delta M_{\mathrm{f}} = \Delta M_{1,2} + \Delta M_{J_{\mathrm{f}}^{(d)},} + \Delta M^{(\mathrm{d})}_{J_{\mathrm{f}}^{(d)}} + \Delta M^{(\mathrm{a})}_{J_{\mathrm{f}}^{(d)}}. \tag{79}$$

Proposition 1 *The following components for effective velocity V_{run} and D_{run} given in (74) and (71) have the explicit forms*

$$\mathbb{E}[\Delta T_{\mathrm{f}}] = \frac{1}{\bar{d}^*_{1,2}} + \frac{p^{(2)}_{d|\mathcal{A}}}{\bar{a}^{*(2)}+\bar{d}^*_1} + \frac{(1-p^{(2)}_{d|\mathcal{A}})}{\bar{a}^{*(1)}+\bar{d}^*_2}, \tag{80}$$

$$\mathbb{E}[\Delta M_{\mathrm{f}}] = \frac{\bar{V}_{1,2}}{\bar{d}^*_{1,2}} + \mu_{R^{(\mathrm{d})}}\left(p^{(2)}_{d|\mathcal{A}} - \frac{\tilde{\kappa}^{(1)}}{2}\right) + \frac{p^{(2)}_{d|\mathcal{A}}\bar{V}_1}{\bar{a}^{*(2)}+\bar{d}^*_1} \tag{81}$$

$$+ \frac{(1-p^{(2)}_{d|\mathcal{A}})\bar{V}_2}{\bar{a}^{*(1)}+\bar{d}^*_2} - \frac{\tilde{F}}{2}\left(p^{(2)}_{d|\mathcal{A}}\frac{\tilde{\kappa}^{(2)}}{\tilde{\kappa}^{(1)}} + (1-p^{(2)}_{d|\mathcal{A}})\frac{\tilde{\kappa}^{(1)}}{\tilde{\kappa}^{(2)}}\right), \tag{82}$$

$$\mathrm{Var}(\Delta T_{\mathrm{f}}) = \frac{1}{(\bar{d}^*_{1,2})^2} + p^{(2)}_{d|\mathcal{A}}\frac{1}{(\bar{a}^{*(2)}+\bar{d}^*_1)^2} + (1-p^{(2)}_{d|\mathcal{A}})\frac{1}{(\bar{a}^{*(1)}+\bar{d}^*_2)^2} \tag{83}$$

$$+ p^{(2)}_{d|\mathcal{A}}(1-p^{(2)}_{d|\mathcal{A}})\left(\frac{1}{(\bar{a}^{*(2)}+\bar{d}^*_1)} - \frac{1}{(\bar{a}^{*(1)}+\bar{d}^*_2)}\right)^2,$$

where $p^{(i)}_{d|\mathcal{A}}$ is given by (76). Furthermore,

$$\mathrm{Var}(\Delta M_{\mathrm{f}}) = \mathrm{Var}(\Delta M_{1,2}) + \mathrm{Var}(\Delta M_{J_{\mathrm{f}}^{(d)},} + \Delta M^{(\mathrm{a})}_{J_{\mathrm{f}}^{(d)}} + \Delta M^{(\mathrm{d})}_{J_{\mathrm{f}}^{(d)}}), \tag{84}$$

$$\mathrm{Cov}(\Delta M_{\mathrm{f}}, \Delta T_{\mathrm{f}}) = \mathbb{E}[\Delta M_{1,2}\Delta T_{1,2}] - \mathbb{E}[\Delta M_{1,2}]\mathbb{E}[\Delta T_{1,2}] \tag{85}$$

$$+ \mathbb{E}[(\Delta M_{J_{\mathrm{f}}^{(d)},} + \Delta M^{(\mathrm{a})}_{J_{\mathrm{f}}^{(d)}} + \Delta M^{(\mathrm{d})}_{J_{\mathrm{f}}^{(d)}})\Delta T_{J_{\mathrm{f}}^{(d)},}] \tag{86}$$

$$- \mathbb{E}[\Delta T_{J_{\mathrm{f}}^{(d)},}]\mathbb{E}[\Delta M_{J_{\mathrm{f}}^{(d)},} + \Delta M^{(\mathrm{a})}_{J_{\mathrm{f}}^{(d)}} + \Delta M^{(\mathrm{d})}_{J_{\mathrm{f}}^{(d)}}] \tag{87}$$

Explicit expressions for the components in (84)-(87) are provided in equations (91)-(94).

We now provide sketches for the calculations in Proposition 1. Beginning with the definition (79) of ΔM_{f} and recalling that conditioning on reattachment $\mathcal{A}$ only affects the probability of which motor detaches first, we obtain the direct modification

$$\mathbb{E}[\Delta M_{\mathrm{f}}] = \frac{\bar{V}_{1,2}}{\bar{d}^*_{1,2}} + p^{(2)}_{d|\mathcal{A}} \left(\frac{\bar{V}_1}{\bar{a}^{*(2)} + \bar{d}^*_1} + \frac{\tilde{\kappa}^{(2)} \mu_{R^{(\mathrm{d})}}}{2} - \frac{\tilde{\kappa}^{(2)} \tilde{F}}{2\tilde{\kappa}^{(1)}} \right) \tag{88}$$

$$+ (1 - p^{(2)}_{d|\mathcal{A}}) \left(\frac{\bar{V}_2}{\bar{a}^{*(1)} + \bar{d}^*_2} - \frac{\tilde{\kappa}^{(1)} \mu_{R^{(\mathrm{d})}}}{2} - \frac{\tilde{\kappa}^{(1)} \tilde{F}}{2\tilde{\kappa}^{(2)}} \right), \tag{89}$$

which is equivalent to (82). A similar argument yields Eq. (80).

To find $\mathrm{Var}(\Delta T_{\mathrm{f}})$, first note that the times spent within the fully attached and one-motor-detached states are independent, which gives

$$\mathrm{Var}(\Delta T_{\mathrm{f}}) = \mathrm{Var}(\Delta T_{1,2}) + \mathrm{Var}(\Delta T_{J^{(d)}_{\mathrm{f}},}), \tag{90}$$

From (57), $\mathrm{Var}(\Delta T_{1,2}) = 1/(\bar{d}^*_{1,2})^2$. For the second term in (90), we use the law of total variance, conditioning over values of $J^{(d)}_{\mathrm{f}}$, to obtain

$$\begin{aligned} &\mathrm{Var}(\Delta T_{J^{(d)}_{\mathrm{f}},}) \\ &= \mathrm{Var}(\Delta T_1) p^{(2)}_{d|\mathcal{A}} + \mathrm{Var}(\Delta T_2)(1 - p^{(2)}_{d|\mathcal{A}}) + \mathbb{E}[(\Delta T_1 - \Delta T_2)^2] p^{(2)}_{d|\mathcal{A}} (1 - p^{(2)}_{d|\mathcal{A}}), \end{aligned}$$

which is equivalent to (83).

To compute (84), we may again partition on possible values of $J^{(d)}_{\mathrm{f}}$, obtaining

$$\mathrm{Var}(\Delta M_{J^{(d)}_{\mathrm{f}},} + \Delta M^{(\mathrm{a})}_{J^{(d)}_{\mathrm{f}}} + \Delta M^{(\mathrm{d})}_{J^{(d)}_{\mathrm{f}}}) \tag{91}$$

$$= (1 - p^{(2)}_{d|\mathcal{A}}) \,\mathrm{Var}(A) + p^{(2)}_{d|\mathcal{A}} \,\mathrm{Var}(B) + p^{(2)}_{d|\mathcal{A}} (1 - p^{(2)}_{d|\mathcal{A}}) (\mathbb{E}[A] - \mathbb{E}[B])^2, \tag{92}$$

where we define

$$A := \Delta M_2 + \Delta M^{(\mathrm{a})}_1 + \Delta M^{(\mathrm{d})}_1, \quad B := \Delta M_1 + \Delta M^{(\mathrm{a})}_2 + \Delta M^{(\mathrm{d})}_2. \tag{93}$$

Computing the variance of A and B is then immediate through independence and (63)-(64).

It remains to calculate the covariance $\mathrm{Cov}(\Delta M_{\mathrm{f}}, \Delta T_{\mathrm{f}})$. The decomposition provided in (85)-(87) is straightforward from applying the definitions (56),

(58), and (93). All terms in (85)-(87) have already been computed, except for

$$\mathbb{E}[\Delta T_{1,2}\Delta M_{1,2}] = \frac{2\bar{V}_{1,2}}{(\bar{d}^*_{1,2})^2}, \tag{94}$$

$$\begin{aligned}
&\mathbb{E}[(\Delta M_{J_{\mathrm{f}}^{(d)},} + \Delta M^{(\mathrm{a})}_{J_{\mathrm{f}}^{(d)}} + \Delta M^{(\mathrm{d})}_{J_{\mathrm{f}}^{(d)}})\Delta T_{J_{\mathrm{f}}^{(d)},}] \\
&= p^{(2)}_{d|\mathcal{A}} \left(\frac{2\bar{V}_1}{(\bar{a}^{*(2)} + \bar{d}^*_1)^2} + \frac{1}{\bar{a}^{*(2)} + \bar{d}^*_1} \left(\frac{1}{2}\tilde{\kappa}^{(2)}\mu_{R^{(\mathrm{d})}} - \frac{\tilde{\kappa}^{(2)}\tilde{F}}{2\tilde{\kappa}^{(1)}} \right) \right) \\
&+ (1 - p^{(2)}_{d|\mathcal{A}}) \left(\frac{2\bar{V}_2}{(\bar{a}^{*(1)} + \bar{d}^*_2)^2} - \frac{1}{\bar{a}^{*(1)} + \bar{d}^*_2} \left(\frac{1}{2}\tilde{\kappa}^{(1)}\mu_{R^{(\mathrm{d})}} + \frac{\tilde{\kappa}^{(1)}\tilde{F}}{2\tilde{\kappa}^{(2)}} \right) \right),
\end{aligned} \tag{95}$$

which are all found through iterated conditioning.

5.2.2 Ensemble Diffusivity

For computing ensemble diffusivity, we must consider statistics related to the condition of a terminal cycle. Under this condition, let the random index $J^{(d)}_{\mathrm{t}} \in \{1, 2\}$ denote which motor detaches from the $(1, 2)$ state, which is computed, similarly to (76), as

$$p^{(i)}_{d|\mathcal{A}^c} := \mathbb{P}(J^{(d)}_{\mathrm{t}} = i) \tag{96}$$

$$= \frac{\frac{\bar{d}^*_{i'}}{\bar{d}^*_{i'} + a^{*(i)}} \left(\frac{\bar{d}^{*(i)}_{1,2}}{\bar{d}^*_{1,2}} \right)}{\frac{\bar{d}^*_{i'}}{\bar{d}^*_{i'} + \bar{a}^{*(i)}} \left(\frac{\bar{d}^{*(i)}_{1,2}}{\bar{d}^*_{1,2}} \right) + \frac{\bar{d}^*_{i}}{\bar{d}^*_{i} + a^{*(i')}} \left(\frac{\bar{d}^{*(i')}_{1,2}}{\bar{d}^*_{1,2}} \right)}. \tag{97}$$

The distributions of run lengths for the terminal cycle are then given by

$$\Delta T_{\mathrm{t}} = \Delta T_{1,2} + \Delta T_{J^{(d)}_{\mathrm{t}},}, \tag{98}$$

$$\Delta M_{\mathrm{t}} = \Delta M_{1,2} + \Delta M_{J^{(d)}_{\mathrm{t}},} + \Delta M^{(\mathrm{d})}_{J^{(d)}_{\mathrm{t}}}. \tag{99}$$

Through the same calculations as Prop. 1, we may compute the same quantities for ΔT_{t} and ΔM_{t} by replacing $p^{(i)}_{d|\mathcal{A}}$ with $p^{(i)}_{d|\mathcal{A}^c}$ and $\Delta M^{(\mathrm{a})}_i$ with 0. For computing ensemble velocity and diffusivity, we must first find expressions related to statistics for ΔT_{c} and ΔM_{c}. However, this is straightforward, as we may simply condition on $\mathcal{A}$, yielding

$$\begin{aligned}
\mathbb{E}[\Delta T_{\mathrm{c}}] &= (1-p)\mathbb{E}[\Delta T_{\mathrm{f}}] + p\mathbb{E}[\Delta T_{\mathrm{t}}], \\
\mathbb{E}[\Delta M_{\mathrm{c}}] &= (1-p)\mathbb{E}[\Delta M_{\mathrm{f}}] + p\mathbb{E}[\Delta M_{\mathrm{t}}], \\
\mathrm{Var}(\Delta T_{\mathrm{c}}) &= (1-p)\,\mathrm{Var}(\Delta T_{\mathrm{f}}) + p\,\mathrm{Var}(\Delta T_{\mathrm{t}}) + p(1-p)(\mathbb{E}[\Delta T_{\mathrm{f}}] - \mathbb{E}[\Delta T_{\mathrm{t}}])^2, \\
\mathrm{Var}(\Delta M_{\mathrm{c}}) &= (1-p)\,\mathrm{Var}(\Delta M_{\mathrm{f}}) + p\,\mathrm{Var}(\Delta M_{\mathrm{t}}) + p(1-p)(\mathbb{E}[\Delta M_{\mathrm{f}}] - \mathbb{E}[\Delta M_{\mathrm{t}}])^2, \\
\mathrm{Cov}(\Delta T_{\mathrm{c}}, \Delta M_{\mathrm{c}}) &= (1-p)\mathbb{E}[\Delta M_{\mathrm{f}}\Delta T_{\mathrm{f}}] + p\mathbb{E}[\Delta M_{\mathrm{t}}\Delta T_{\mathrm{t}}] - \mathbb{E}[\Delta T_{\mathrm{c}}]\mathbb{E}[\Delta M_{\mathrm{c}}]
\end{aligned}$$

We thus have explicit expressions for the mean and variance of T and $M(T)$, given in (66)-(68).

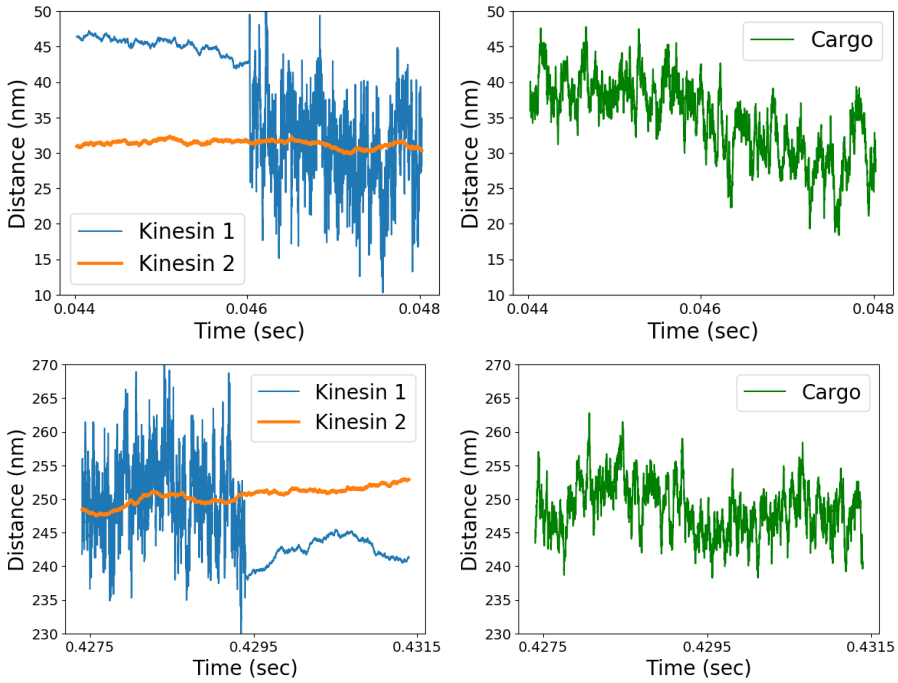

Fig. 4: Switching behavior for a sample path of the kinesin-1/kinesin-2 complex simulation using double exponential detachment rate functions and parameters taken from Table 1. Top left: Motor behavior at an attachment event, with kinesin 2 (thick orange) attached at all times shown, and kinesin 1 (thin blue) attaching near $t = .046$. Top right: Behavior of cargo during at an attachment event. Bottom left: Motor behavior at a detachment event, with kinesin 2 (thick orange) attached at all times shown, and kinesin 1 (thin blue) detaching near $t = .4295$. Bottom right: Behavior of cargo during at a detachment event.

6 Simulations

In this section, we compare theoretical and sample statistics through direct simulation of equations (1)-(5) for two motor ensembles. Both homogeneous (kinesin 1/kinesin 1 or kinesin 2/kinesin 2) and heterogeneous (kinesin 1/kinesin 2) emsembles are simulated, using the parameters in Table 1. For each ensemble, we consider laser trap strengths of $F_T = -5, 0$,and 5 pN. We also considered two separate detachment models. The first utilizes a double exponential function, in which

$$d^{(i)}(F) = \begin{cases} d_0^{-(i)} \exp(-F\delta^{-(i)}/k_B T) & F \leq 0, \\ d_0^{+(i)} \exp(F\delta^{+(i)}/k_B T) & F > 0. \end{cases} \tag{100}$$

Parameter	Kinesin 1 ($i = 1$)	Kinesin 2 ($i = 2$)	Reference
$a^{(i)}$	4/s	16/s	Feng et al. [14]
$d_0^{-(i)}$	0.6/s	2.3/s	Milic et al. [16,17]
$d_0^{+(i)}$	8.1/s	5.6/s	Milic et al. [16,17]
$\delta^{-(i)}$	2.0 nm	2.1 nm	Milic et al. [16,17]
$\delta^{+(i)}$	0.3 nm	0.4 nm	Milic et al. [16,17]

Table 3: Parameters of detachment and attachment for kinesin 1 and 2.

We also use constant detachment rates, in which case we use $d^{(i)}(F) \equiv \bar{d}_i^*$. In all cases, we used constant values $a^{(i)}$ for attachment rates. Values of parameters related to attachment and detachment are found in Table 3.

Between attachment and detachment events, (1)-(3) is simulated by an Euler-Maruyama discretization with a time increment $\Delta t = 10^{-6}s$. With the same time increment, we also discretized the random switching processes by time-dependent Bernoulli processes. Our choice of the force-velocity curve g is the same used in [23], defined by

$$g(x) = A - B\tanh(Cx - D), \tag{101}$$

with $g(x) \to 1.2$ as $x \to -\infty$ and $g(x) \to -.1$ as $x \to \infty$. With the requirements $g(0) = 1$ and $g(1) = 0$, the constants A, B, C, and D may be uniquely determined.

For each motor ensemble, detachment model, and trap force strength considered, we simulated 6,000 runs, each of which beginning with two attached motors and ending with complete detachment. To collect sample statistics for V_{pool} and D_{pool}, we used the estimators

$$\hat{V}^S_{\text{pool}} \equiv \frac{\sum_{j=1}^S M(T^j)}{\sum_{j=1}^S T^j}, \tag{102}$$

$$\hat{D}^S_{\text{pool}} \equiv \frac{\left(\sum_{j=1}^S (M(T^j) - V_{\text{pool}} T^j)\right)^2}{2\sum_{j=1}^S T^j}. \tag{103}$$

We fixed $S = 20$ runs for each sample mean and diffusion. For the V_{pool} term in (103), we estimated using (102) with 1000 runs. These runs are separate from the S runs used in calculating each sample diffusivity. For D_{run} and D_{pool}, we restricted runs to those with at least four full cycles.

Results from simulations are given in Table 4 for constant detachment rates and Table 5 for double exponential detachment rates. The closest agreement occurs with constant detachment models, homogeneous systems, and zero trap forces. For the model whose sample statistics deviate the most from theoretical values, the kinesin 1/kinesin 2 ensemble with double exponential detachment and $F_T = -5$, we note the separation of scales no longer holds, as $\bar{d}^* \approx 1$. Thus, after switching from state (1) or (2) to (1,2), attached motors may not have enough time to equilibrate. This effect is magnified in the case of heterogeneous

	Kinesin 1/Kinesin 1					
	$F_T = -5$		$F_T = 0$		$F_T = 5$	
	Simulation	**Theory**	**Simulation**	**Theory**	**Simulation**	**Theory**
V_{run}	952.60 ± 2.33	940.57	754.55 ± 2.23	753.52	261.75 ± 2.87	272.36
V_{pool}	970.23 ± 1.47	940.57	755.98 ± 1.33	753.52	249.29 ± 1.67	272.36
D_{run}	2041.21 ± 236.21	2511.83	1953.14 ± 244.34	2095.46	3219.13 ± 373.37	3428.44
D_{pool}	2781.72 ± 22.56	2502.21	2324.18 ± 217.17	2095.46	3437.01 ± 274.08	3428.44
N_{c}	$2.06 \pm .02$	2.04	$2.06 \pm .02$	2.05	$2.05 \pm .02$	2.05
T	$.43 \pm .005$	.42	$.43 \pm .005$	.42	$.42 \pm .005$	.42
$M(T)$	414.04 ± 4.42	398.07	321.86 ± 3.68	318.91	105.79 ± 1.55	115.27
	Kinesin 2/Kinesin 2					
V_{run}	665.87 ± 1.34	652.06	$483.63 \pm .91$	482.87	125.29 ± 1.36	145.13
V_{pool}	676.99 ± 1.11	652.06	$484.17 \pm .78$	482.87	116.51 ± 1.09	145.13
D_{run}	1368.30 ± 210.97	1122.06	670.82 ± 95.22	679.47	1366.01 ± 244.90	1239.16
D_{pool}	1562.83 ± 135.14	1122.06	688.67 ± 65.73	679.47	1422.21 ± 127.37	1239.16
N_{c}	$3.38 \pm .04$	3.39	$3.39 \pm .04$	3.39	$3.35 \pm .04$	3.39
T	$.40 \pm .005$	.40	$.40 \pm .005$	.40	$.40 \pm .005$	.40
$M(T)$	272.40 ± 3.03	262.75	194.45 ± 2.29	194.58	$47.20 \pm .89$	58.48
	Kinesin 1/Kinesin 2					
V_{run}	761.06 ± 2.30	698.59	590.27 ± 1.65	562.24	203.24 ± 1.73	210.07
V_{pool}	759.83 ± 1.61	678.88	578.34 ± 1.13	550.31	190.03 ± 1.25	204.39
D_{run}	4304.25 ± 404.42	3852.19	2114.30 ± 188.58	2047.55	2323.70 ± 200.09	2162.21
D_{pool}	3727.65 ± 336.08	3504.65	1796.08 ± 161.95	1917.45	2336.98 ± 196.80	2142.71
N_{c}	$2.80 \pm .03$	2.78	$2.79 \pm .03$	2.78	$2.82 \pm .03$	2.78
T	$.50 \pm .006$	.50	$.50 \pm .006$	.50	$.50 \pm .006$	.50
$M(T)$	378.57 ± 4.21	342.41	290.60 ± 3.45	277.81	96.28 ± 1.46	103.09

Table 4: Simulation and theoretical statistics with constant detachment rates. Error bars denote one sample standard deviation.

ensembles, in which there is a large expected intermotor distance. In the double exponential model with $F_T = -5$, for example, we have $\mu_{R^{(\text{d})}} = 45.28$ nm. See Fig. 4 for a visualization of attachment and detachment events of a kinesin 1/kinesin 2 ensemble.

7 Conclusion

We have modeled transport of multiple, nonidentical molecular motors along a microtubule. Transport is governed through several systems of continuous SDEs, Cox processes, a generalization of inhomogeneous Poisson processes, are used to determine attachment and detachment times of individual motors. After a nondimensionalization of the governing equations and rate functions, we produced averaging formulas for motor positions. In the case of two motor systems, we have produced effective one-dimensional SDEs for the expected cargo position. Considered with jumping behavior at switching events, we then derived formulas effective velocity, diffusion, and mean run length.

A Time-Change Representation of Coarse-Grained Markov Chain Model

We can formalize the description of the coarse-grained Markov chain dynamics in Subsection 4.3 through the association of standard Poisson counting processes with each potential

	Kinesin 1/Kinesin 1					
	$F_T = -5$		$F_T = 0$		$F_T = 5$	
	Simulation	**Theory**	**Simulation**	**Theory**	**Simulation**	**Theory**
V_{run}	993.97 ± 22.56	959.51	738.18 ± 18.12	754.04	190.19 ± 10.73	224.58
V_{pool}	1017.35 ± 1.29	959.51	734.26 ± 1.10	754.04	148.08 ± 0.96	224.58
D_{run}	2543.97 ± 190.24	3202.90	2094.53 ± 219.31	2173.71	4465.50 ± 279.26	3003.71
D_{pool}	3043.87 ± 541.20	3202.90	2205.80 ± 178.27	2173.71	3746.49 ± 360.42	3003.71
N_{c}	$1.65 \pm .01$	1.64	$2.06 \pm .02$	2.05	$1.44 \pm .01$	1.43
T	$.30 \pm .003$	.25	$.46 \pm .005$	.41	$.16 \pm .002$	.16
$M(T)$	302.22 ± 2.99	240.47	298.52 ± 3.49	311.86	$250.55 \pm .60$	367.30
	Kinesin 2/Kinesin 2					
V_{run}	915.30 ± 12.47	761.11	$483.61 \pm .67$	482.50	109.76 ± 1.79	140.67
V_{pool}	930.15 ± 3.29	761.11	$483.08 \pm .61$	482.50	95.25 ± 1.41	140.67
D_{run}	3902.97 ± 210.32	2380.57	654.80 ± 95.44	684.44	1497.25 ± 245.34	1244.91
D_{pool}	3588.79 ± 287.10	2380.57	638.35 ± 58.25	684.44	1785.34 ± 155.72	1244.91
N_{c}	$1.48 \pm .01$	1.47	$4.25 \pm .05$	4.28	$2.77 \pm .03$	2.75
T	$.09 \pm .001$	.08	$.60 \pm .007$	.61	$.31 \pm .004$	.30
$M(T)$	$85.56 \pm .69$	58.06	290.38 ± 3.50	292.92	$29.79 \pm .67$	42.56
	Kinesin 1/Kinesin 2					
V_{run}	970.37 ± 3.22	1463.34	595.72 ± 1.92	584.51	135.03 ± 3.90	153.83
V_{pool}	1015.06 ± 2.41	1431.66	581.74 ± 1.41	563.35	102.17 ± 2.22	148.80
D_{run}	2140.62 ± 230.61	9486.46	2283.88 ± 197.63	3365.51	2428.40 ± 311.92	1960.06
D_{pool}	3531.95 ± 316.83	9552.91	2259.96 ± 220.23	3126.07	2870.49 ± 273.15	1911.34
N_{c}	$2.21 \pm .02$	2.76	$2.71 \pm .03$	2.88	$1.78 \pm .02$	1.78
T	$.20 \pm .002$	.13	$.40 \pm .005$	.37	$.21 \pm .002$	.21
$M(T)$	207.00 ± 2.16	194.71	234.46 ± 2.73	210.31	22.10 ± 5.60	31.67

Table 5: Simulation and theoretical statistics with double exponential detachment rates. Error bars denote one sample standard deviation.

state transition. We thereby define, with associations, the standard Poisson counting processes $Y_i^{(1,2)}(t)$ to represent detachment of motor i from the two-motor attached state, and $Y_d^{(i)}(t)$ to represent detachment of motor i when it is the only motor attached, and $Y_a^{(i')}(t)$ to represent attachment of motor i when only motor $i' = 3 - i$ is attached. Then the dynamics of the attachment states can be written, for $i = 1, 2$, as

$$dB^{(i)}(t) = Y_a^{(i')}\left(\bar{a}^{*(i')}\int_0^t (1 - B^{(i)}(t'))B^{(i')}(t')dt'\right) \tag{104}$$

$$- Y_i^{(1,2)}\left(\bar{d}_{1,2}^{*(i)}\int_0^t B^{(1)}(t')B^{(2)}(t')dt'\right) - Y_d^{(i)}\left(\bar{d}_i^*\int_0^t B^{(i)}(t')(1 - B^{(i')}(t'))dt'\right), \tag{105}$$

while the dynamics of the tracking variable can be written as

$$dM(t) = B^{(1)}(t)B^{(2)}(t)(\bar{V}_{1,2}dt + \sqrt{2D^{(1,2)}}dW(t)) \tag{106}$$

$$+ \sum_{j=1}^{2} B^{(j)}(t)(1 - B^{(j')}(t))(\bar{V}_j dt + \sqrt{\rho^{(j)}}dW^{(j)}(\bar{t}))$$

$$+ \sum_{j=1}^{2}\left(\frac{\tilde{\kappa}^{(j')}(-1)^j}{2}R^j_{Y_j^{(1,2)}\left(\bar{d}_{1,2}^{*(j)}\int_0^t B^{(1)}(t')B^{(2)}(t')dt'\right)} - \frac{\tilde{\kappa}^{(j')}\tilde{F}}{2\tilde{\kappa}^{(j)}}\right)\cdot Y_j^{(1,2)}\left(\bar{d}_{1,2}^{*(j)}\int_0^t B^{(1)}(t')B^{(2)}(t')dt'\right)$$

$$+ \sum_{j=1}^{2}\left(\frac{1}{2}\sqrt{\frac{\tilde{\kappa}^{(j')}}{\tilde{\kappa}^{(j)}}}\xi^j_{Y_a^{(j)}\left(\bar{a}^{*(j')}\int_0^t B^{(j)}(t')(1-B^{(j')}(t'))dt'\right)}\right)\cdot Y_a^{(j)}\left(\bar{a}^{*(j')}\int_0^t B^{(j)}(t')(1 - B^{(j')}(t'))dt'\right).$$

Here, R_j^1, R_j^2, ξ_j^1 and ξ_j^2, $j \geq 1$ are iid streams of random variables, where $R_1^1, R_1^2 \sim R^{\text{det}}$ and ξ_1, ξ_2 are standard normal random variables.

B A note on nonlinear spring models

A linear model for representing the tether between the motor and the cargo is not particularly accurate. Better theoretical tether models can involve a model which is Hookean for extension beyond a rest length, but offers no resistance to compression, a sigmoidal stiffness dependence on force, or a multiple-component model for the motor-cargo tether including separate models for the neck linker and stalk.

We may generalize the averaging results by considering a nonlinear spring

$$F^{(i)}(r) = \bar{F}^{(i)}\Phi'^{(i)}(r/L_c) \quad 1 \leq i \leq N. \tag{107}$$

Here $\Phi^{(i)}(r)$ is a nondimensionalized spring potential, L_c is an appropriate length scale, and $\bar{F}^{(i)}$ is a characteristic magnitude. Here, we will assume that the force is linear under small displacements up to L_c, so that we may write $\bar{F} = \kappa^{(i)} L_c$. With the same nondimensionalization as before, the equations of motion become

$$d\tilde{X}^{(i)}(\tilde{t}) = \left(\epsilon^{(i)} g(s^{(i)}\lambda^{-1}\Phi'^{(i)}(\lambda(\tilde{X}^{(i)}(\tilde{t}) - \tilde{Z}(\tilde{t})))d\tilde{t} + \sqrt{\hat{\rho}^{(i)}\epsilon^{(i)}}dW^{(i)}(\tilde{t})\right) B^{(i)}(t) \tag{108}$$

$$+ \left(-(\Gamma^{(i)})^{-1}\kappa^{(i)}(\tilde{X}^{(i)}(\tilde{t}) - \tilde{Z}(\tilde{t}))d\tilde{t} + \sqrt{(\Gamma^{(i)})^{-1}}dW^{(i)}(\tilde{t})\right)(1 - B^{(i)}(t)), \quad 1 \leq i \leq N,$$

$$d\tilde{Z}(\tilde{t}) = \left(\sum_{j=1}^{N} \lambda^{-1}\Phi'(\lambda(\tilde{X}^{(j)}(\tilde{t}) - \tilde{Z}(\tilde{t}))) - \tilde{F}_T\right) d\tilde{t} + dW_z(\tilde{t}), \tag{109}$$

where we have introduced the new nondimensional parameter

$$\lambda = \frac{\sqrt{2k_B T/\bar{\kappa}}}{L_c}. \tag{110}$$

Calculations for the averaged drifts $\bar{g}^{(i)}$, and thus G_+ and G_-, are similar, but now involve pairing drift functions with non-Gaussian stationary distributions for unattached motors and cargo (the forms for these equations are nearly identical to those found in Appendix A in [23]). Subsequently, the random variable $\Delta M_i^{(\mathrm{a})}$ describing the change of position after motor attachment, derived in Section 4.2 , is no longer normal. After deriving effective SDEs for one and two attached motor ensembles, effective velocity and diffusion for two motor ensembles with switching may then be found through the same renewal theory arguments provided in Section 5, although several moments will not have explicit expressions as before (e.g. $\mathbb{E}[\Delta C^{(1)}]$ may be nonzero, as the distribution for jumps size at attachment may not be symmetric about 0).

C Derivation of effective diffusion for two motors

The following derivation for the effective diffusion of the cargo tracking variable during a state with both motors attached to the microtubule follows the multiscale expansion method illustrated in Pavliotis [39]. Having computed the effective drift $\bar{V}_{1,2}$ in Eq. (41) in this state, we pass to a diffusive scaling centered about this mean drift $\bar{t} \to t/\epsilon^2$, $M \to \epsilon(M - \bar{V}_{1,2}t)$, with the internal configuration variable R unscaled ($R \to R$). Note in this appendix, ϵ is just a formal small parameter used to push to long time; it is unrelated to the physically meaningful nondimensional parameters $\epsilon^{(i)}$ and $\bar{\epsilon}$ in the main text. Moreover, for simplicity for calculations within this appendix, we use the undecorated variables t, M, R to describe the dynamics under this centered diffusive rescaling, which read:

$$dM(t) = \frac{1}{\varepsilon}\left(G_+(R(t)) - \bar{V}_{1,2}\right)dt + \frac{\sqrt{\rho^{(1)}(\tilde{\kappa}^{(1)})^2}}{2}dW^{(1)}(t) + \frac{\sqrt{\rho^{(2)}(\tilde{\kappa}^{(2)})^2}}{2}dW^{(2)}(t) \tag{111}$$

$$dR(t) = \frac{1}{\varepsilon^2}G_-(R(t))dt + \frac{1}{\varepsilon}\left(\sqrt{\rho^{(1)}}dW^{(1)}(t) - \sqrt{\rho^{(2)}}dW^{(2)}(t)\right). \tag{112}$$

The infinitesimal generator $\mathcal{L}$ for (111)-(112) is defined by its action on a test function $v = v(m, r)$, with

$$\mathcal{L}v(m,r) = \mathbf{h} \cdot \nabla v + \frac{1}{2} \Gamma : \nabla\nabla v. \tag{113}$$

Here $\mathbf{h}(m,r) = ((G_+(r) - \bar{V}_{1,2})/\varepsilon, G_-(r)/\varepsilon^2)$ is the drift vector, and $\frac{1}{2}\Gamma$ is the diffusion tensor, where

$$\Gamma = \begin{bmatrix} \frac{\sqrt{\rho^{(1)}(\tilde{\kappa}^{(1)})^2}}{2} & \frac{\sqrt{\rho^{(2)}(\tilde{\kappa}^{(2)})^2}}{2} \\ \frac{\sqrt{\rho^{(1)}}}{\varepsilon} & -\frac{\sqrt{\rho^{(2)}}}{\varepsilon} \end{bmatrix} \begin{bmatrix} \frac{\sqrt{\rho^{(1)}(\tilde{\kappa}^{(1)})^2}}{2} & \frac{\sqrt{\rho^{(2)}(\tilde{\kappa}^{(2)})^2}}{2} \\ \frac{\sqrt{\rho^{(1)}}}{\varepsilon} & -\frac{\sqrt{\rho^{(2)}}}{\varepsilon} \end{bmatrix}^T \tag{114}$$

$$= \begin{bmatrix} \frac{\rho^{(1)}(\tilde{\kappa}^{(1)})^2 + \rho^{(2)}(\tilde{\kappa}^{(2)})^2}{4} & \frac{\rho^{(1)}\tilde{\kappa}^{(1)} - \rho^{(2)}\tilde{\kappa}^{(2)}}{2\varepsilon} \\ \frac{\rho^{(1)}\tilde{\kappa}^{(1)} - \rho^{(2)}\tilde{\kappa}^{(2)}}{2\varepsilon} & \frac{\rho^{(1)} + \rho^{(2)}}{\varepsilon^2} \end{bmatrix}. \tag{115}$$

We may write out (113) explicitly as

$$\mathcal{L}v(m,r) = \mathbf{h} \cdot \nabla v + \frac{1}{2} \Gamma : \nabla\nabla v \tag{116}$$

$$= \frac{1}{\varepsilon}(G_+(r) - \bar{V}_{1,2}) v_m + \frac{1}{\varepsilon^2} G_-(r) v_r \tag{117}$$

$$+ \frac{1}{2}\left[\left(\frac{\rho^{(1)}(\tilde{\kappa}^{(1)})^2 + \rho^{(2)}(\tilde{\kappa}^{(2)})^2}{4} \right) v_{mm} + \frac{\rho^{(1)}\tilde{\kappa}^{(1)} - \rho^{(2)}\tilde{\kappa}^{(2)}}{\varepsilon} v_{mr} + \left(\frac{\rho^{(1)} + \rho^{(2)}}{\varepsilon^2} \right) v_{rr} \right]. \tag{118}$$

The generator may be decomposed to match powers of ε as

$$\mathcal{L} = \frac{1}{\varepsilon^2}\mathcal{L}_0 + \frac{1}{\varepsilon}\mathcal{L}_1 + \mathcal{L}_2, \tag{119}$$

with

$$\mathcal{L}_0 = G_-(r)\partial_r + \frac{\rho^{(1)} + \rho^{(2)}}{2}\partial_{rr}, \tag{120}$$

$$\mathcal{L}_1 = \frac{\rho^{(1)}\tilde{\kappa}^{(1)} - \rho^{(2)}\tilde{\kappa}^{(2)}}{2}\partial_{mr} + \left(G_+(r) - \bar{V}_{1,2}\right)\partial_m, \tag{121}$$

$$\mathcal{L}_2 = \left(\frac{\rho^{(1)}(\tilde{\kappa}^{(1)})^2 + \rho^{(2)}(\tilde{\kappa}^{(2)})^2}{8} \right)\partial_{mm}. \tag{122}$$

Assuming a multiscale solution $v = v_0 + \varepsilon v_1 + \varepsilon^2 v_2 + \dots$ for the backward Kolmogorov equation

$$\frac{\partial v}{\partial t} = \mathcal{L}v, \tag{123}$$

we match powers of orders $1/\varepsilon^2, 1/\varepsilon$, and 1 to obtain

$$\mathcal{L}_0 v_0 = 0, \tag{124}$$

$$-\mathcal{L}_0 v_1 = \mathcal{L}_1 v_0, \tag{125}$$

$$-\mathcal{L}_0 v_2 = -\frac{\partial v_0}{\partial t} + \mathcal{L}_1 v_1 + \mathcal{L}_2 v_0. \tag{126}$$

The first equation implies that v_0 is only a function of m and t. From here, the second equation may be simplified to

$$-\mathcal{L}_0 v_1 = \left(G_+(r) - \bar{V}_{1,2}\right)\partial_m v_0(m,t). \tag{127}$$

As the operator $\mathcal{L}_0$ only depends on r, we may express v_1 as

$$v_1(m,r,t) = \chi(r)\partial_m v_0(m,t). \tag{128}$$

Proceeding to the third equation of the asymptotic expansion, the Fredholm alternative states that for (126) to have a solution, its right hand side must be orthogonal to $p_R(r)$, or

$$\frac{\partial v_0}{\partial t} = \int_{\mathbb{R}} p_R(r)\mathcal{L}_2 v_0(m,t)dr + \int_{\mathbb{R}} p_R(r)\mathcal{L}_1(\chi(r)\partial_m v_0(m,t))dr \tag{129}$$

$$:= I_1 + I_2. \tag{130}$$

We look at each integral in turn. First,

$$I_1 = \int_{\mathbb{R}} p_R(r)\mathcal{L}_2 v_0(m,t)dr \tag{131}$$

$$= \int_{\mathbb{R}} p_R(r)\left[\left(G_+(r) - \bar{V}_{1,2}\right)\partial_m v_0(m,t) + \left(\frac{\rho^{(1)}(\tilde{\kappa}^{(1)})^2 + \rho^{(2)}(\tilde{\kappa}^{(2)})^2}{8}\right)\partial_{mm} v_0(m,t)\right]dr \tag{132}$$

$$= \left(\frac{\rho^{(1)}(\tilde{\kappa}^{(1)})^2 + \rho^{(2)}(\tilde{\kappa}^{(2)})^2}{8}\right)\partial_{mm} v_0(m,t). \tag{133}$$

The second integral may be broken up further, as

$$I_2 = \int_{\mathbb{R}} p_R(r)\mathcal{L}_1(\chi(r)\partial_m v_0(m,t))dr \tag{134}$$

$$= \int_{\mathbb{R}} p_R(r)\Big[\left(\frac{\rho^{(1)}\kappa^{(1)} - \rho^{(2)}\kappa^{(2)}}{2}\right)\partial_{mr}(\chi(r)\partial_m v_0(m,t)) \tag{135}$$

$$+ \left(G_+(r) - \bar{V}_{1,2}\right)\partial_m(\chi(r)\partial_m v_0(m,t))\Big]dr \tag{136}$$

$$:= I_3 + I_4. \tag{137}$$

The first part satisfies

$$I_3 = \int_{\mathbb{R}} p_R(r)\left(\frac{\rho^{(1)}\tilde{\kappa}^{(1)} - \rho^{(2)}\tilde{\kappa}^{(2)}}{2}\right)\partial_{mr}(\chi(r)\partial_m v_0(m,t))dr \tag{138}$$

$$= \left(\left(\frac{\rho^{(1)}\tilde{\kappa}^{(1)} - \rho^{(2)}\tilde{\kappa}^{(2)}}{2}\right)\int_{\mathbb{R}} p_R(r)\partial_r\chi(r)dr\right)\partial_{mm} v_0(m,t) \tag{139}$$

$$:= A_1\partial_{mm} v_0(m,t). \tag{140}$$

Finally, we have

$$I_4 = \int_{\mathbb{R}} p_R(r)\left[\left(G_+(r) - \bar{V}_{1,2}\right)\partial_m(\chi(r)\partial_m v_0(m,t))\right]dr \tag{141}$$

$$= \int_{\mathbb{R}} p_R(r)\left[\left(G_+(r) - \bar{V}_{1,2}\right)\chi(r)\right]dr\partial_{mm} v_0(m,t) \tag{142}$$

$$:= A_2\partial_{mm} v_0(m,t). \tag{143}$$

The closed form equation for $v_0(m,t)$ is thus given by

$$\frac{\partial v_0}{\partial t} = \frac{1}{2}\left(\frac{\rho^{(1)}(\tilde{\kappa}^{(1)})^2 + \rho^{(2)}(\tilde{\kappa}^{(2)})^2}{4} + 2A_1 + 2A_2\right)\partial_{mm} v_0(m,t), \tag{144}$$

and is the backward Kolmogorov equation for the SDE

$$d\bar{M}(t) = \sqrt{\frac{\rho^{(1)}(\tilde{\kappa}^{(1)})^2 + \rho^{(2)}(\tilde{\kappa}^{(2)})^2}{4} + 2A_1 + 2A_2}dW(t) \tag{145}$$

$$\equiv \sqrt{2D^{(1,2)}}dW(t), \tag{146}$$

where $W(t)$ is a standard Brownian motion. Recall that in this calculation we have recentered the cargo tracking variable $\bar{M}$ about its mean drift dynamics; that drift is restored in the long-time dynamics (REF) of the actual cargo tracking variable in the main text.

Now we compute explicit expressions for constants A_1 and A_2. This involves solving the cell problem for χ, given by

$$-G_-(r)\chi'(r) - \left(\frac{\rho^{(1)}+\rho^{(2)}}{2}\right)\chi''(r) = \tilde{g}_+(r), \tag{147}$$

$$\int_{\mathbb{R}} \chi(r)p_R(r)dr = 0, \tag{148}$$

where we define $\tilde{g}_+(r) = G_+(r) - \bar{V}_{1,2}$. If we rewrite (147), using an integration factor $\mu(r)$, as

$$[\mu(r)\chi'(r)]' = -\mu(r)\tilde{g}_+(r)\left(\frac{2}{\rho^{(1)}+\rho^{(2)}}\right), \tag{149}$$

then it is straightforward to show that $\mu(r)$ is in fact equal to the stationary distribution $p_R(r)$.

Integrating out (149) leaves us with

$$\chi'(r) = -\int_{-\infty}^{r} \tilde{g}_+(r')\left(\frac{2}{\rho^{(1)}+\rho^{(2)}}\right)p_R(r')dr'/p_R(r) + C/p_R(r) \tag{150}$$

for some unknown integration constant C. Assuming subexponential growth of χ and χ'

$$A_1 = \left(\frac{\rho^{(2)}\tilde{\kappa}^{(2)} - \rho^{(1)}\tilde{\kappa}^{(1)}}{\rho^{(1)}+\rho^{(2)}}\right)\int_{\mathbb{R}}\int_{-\infty}^{r} \tilde{g}_+(r')p_R(r')dr'dr \tag{151}$$

$$= \left(\frac{\rho^{(1)}\tilde{\kappa}^{(1)} - \rho^{(2)}\tilde{\kappa}^{(2)}}{\rho^{(1)}+\rho^{(2)}}\right)\int_{\mathbb{R}} \tilde{g}_+(r)p_R(r)\cdot r dr. \tag{152}$$

The last equality used integration by parts, in which the boundary term vanishes under the assumption that $p_R(r) = o(1/r^2)$ as $r \to \pm\infty$. The calculation for A_2 (REF) follows from integration by parts, with

$$A_2 = \int_{-\infty}^{\infty} \chi(r)\tilde{g}_+(r)p_R(r)dr = -\int_{-\infty}^{\infty} \chi(r)(\mathcal{L}_0\chi(r))p_R(r)dr \tag{153}$$

$$= -\int_{-\infty}^{\infty} \chi(r)\left(G_-(r)\chi'(r) + \left(\frac{\rho^{(1)}+\rho^{(2)}}{2}\right)\chi''(r)\right)p_R(r)dr \tag{154}$$

$$= \int_{-\infty}^{\infty}\left(\frac{\rho^{(1)}+\rho^{(2)}}{2}\right)\chi'(r)^2 p_R(r)dr \tag{155}$$

$$= \int_{-\infty}^{\infty}\left(\frac{2}{\rho^{(1)}+\rho^{(2)}}\right)\left(\int_{-\infty}^{r}\tilde{g}_+(r')p_R(r')dr'\right)^2\frac{1}{p_R(r)}dr. \tag{156}$$

References

1. B. Alberts, Molecular Biology of the Cell (CRC Press, 2017). URL https://books.google.com/books?id=2xIwDwAAQBAJ
2. R. Phillips, J. Kondev, J. Theriot, H. Garcia, Physical biology of the cell (Garland Science, 2012)
3. W.O. Hancock, J. Howard, Molecular motors pp. 243–269 (2003)
4. Z. Wang, M. Li, Physical Review E **80**(4), 041923 (2009)
5. A. Kunwar, S.K. Tripathy, J. Xu, M.K. Mattson, P. Anand, R. Sigua, M. Vershinin, R.J. McKenney, C.Y. Clare, A. Mogilner, et al., Proceedings of the National Academy of Sciences **108**(47), 18960 (2011)

6. M.J. Müller, S. Klumpp, R. Lipowsky, Proceedings of the National Academy of Sciences **105**(12), 4609 (2008)
7. R. Mallik, A.K. Rai, P. Barak, A. Rai, A. Kunwar, Trends in cell biology **23**(11), 575 (2013)
8. W.O. Hancock, Nature reviews Molecular cell biology **15**(9), 615 (2014)
9. A.T. Lombardo, S.R. Nelson, M.Y. Ali, G.G. Kennedy, K.M. Trybus, S. Walcott, D.M. Warshaw, Nature communications **8**, 15692 (2017)
10. A.K. Rai, A. Rai, A.J. Ramaiya, R. Jha, R. Mallik, Cell **152**(1-2), 172 (2013)
11. J.D. Smith, S.A. McKinley, Bulletin of mathematical biology pp. 1–36 (2018)
12. M.J. Müller, S. Klumpp, R. Lipowsky, Journal of Statistical Physics **133**(6), 1059 (2008)
13. S. Klumpp, R. Lipowsky, Proceedings of the National Academy of Sciences of the United States of America **102**(48), 17284 (2005)
14. Q. Feng, K.J. Mickolajczyk, G.Y. Chen, W.O. Hancock, Biophysical journal **114**(2), 400 (2018)
15. J.A. Spudich, S.E. Rice, R.S. Rock, T.J. Purcell, H.M. Warrick, Cold Spring Harbor Protocols **2011**(11), pdb (2011)
16. B. Milic, J.O. Andreasson, W.O. Hancock, S.M. Block, Proceedings of the National Academy of Sciences **111**(39), 14136 (2014)
17. B. Milic, J.O. Andreasson, D.W. Hogan, S.M. Block, Proceedings of the National Academy of Sciences **114**(33), E6830 (2017)
18. J.O. Andreasson, S. Shastry, W.O. Hancock, S.M. Block, Current Biology **25**(9), 1166 (2015)
19. C. Leduc, O. Campàs, K.B. Zeldovich, A. Roux, P. Jolimaitre, L. Bourel-Bonnet, B. Goud, J.F. Joanny, P. Bassereau, J. Prost, Proceedings of the National Academy of Sciences of the United States of America **101**(49), 17096 (2004)
20. S.M. Block, L.S. Goldstein, B.J. Schnapp, Nature **348**(6299), 348 (1990)
21. R.D. Vale, T. Funatsu, D.W. Pierce, L. Romberg, Y. Harada, T. Yanagida, Nature **380**(6573), 451 (1996)
22. A. Kunwar, A. Mogilner, Physical biology **7**(1), 016012 (2010)
23. S.A. McKinley, A. Athreya, J. Fricks, P.R. Kramer, Journal of theoretical biology **305**, 54 (2012)
24. J.E. Baker, D.D. Thomas, Biophysical journal **79**(4), 1731 (2000)
25. A. Kunwar, M. Vershinin, J. Xu, S.P. Gross, Current biology **18**(16), 1173 (2008)
26. D. Materassi, M. Salapaka, S. Roychowdhury, T. Hays, BMC biophysics **6**(1), 14 (2013)
27. S. Talukdar, S. Bhaban, D. Materassi, M. Salapaka, in Decision and Control (CDC), 2016 IEEE 55th Conference on (IEEE, 2016), pp. 3356–3362
28. J. Hughes, W.O. Hancock, J. Fricks, Bulletin of mathematical biology **74**(5), 1066 (2012)
29. G.I. Bell, et al., Science **200**(4342), 618 (1978)
30. D.R. Cox, V. Isham, Point processes, vol. 12 (CRC Press, 1980)
31. P.C. Bressloff, J.M. Newby, Physical Review E **83**(6), 061139 (2011)
32. K. Visscher, M.J. Schnitzer, S.M. Block, Nature **400**(6740), 184 (1999)
33. S. Shastry, W. Hancock, Biophysical Journal **98**(3), 369a (2010)
34. G. Muthukrishnan, Y. Zhang, S. Shastry, W.O. Hancock, Current Biology **19**(5), 442 (2009)
35. H. Kojima, E. Muto, H. Higuchi, T. Yanagida, Biophysical Journal **73**(4), 2012 (1997)
36. K. Furuta, A. Furuta, Y.Y. Toyoshima, M. Amino, K. Oiwa, H. Kojima, Proceedings of the National Academy of Sciences **110**(2), 501 (2013)
37. C.C. Lin, L.A. Segel, Mathematics applied to deterministic problems in the natural sciences (SIAM, 1988)
38. I.V. Novozhilov, Fractional analysis: Methods of motion decomposition (Springer Science & Business Media, 2012)
39. G. Pavliotis, A. Stuart, Multiscale methods: averaging and homogenization (Springer Science & Business Media, 2008)
40. A.V. Skorokhod, F.C. Hoppensteadt, H.D. Salehi, Random perturbation methods with applications in science and engineering, vol. 150 (Springer Science & Business Media, 2002)
41. R. Liptser, J. Stoyanov, Stochastics: An International Journal of Probability and Stochastic Processes **32**(3-4), 145 (1990)

42. S. Bouzat, Physical Review E **93**(1), 012401 (2016)
43. Y.A. Kutoyants, Statistical inference for ergodic diffusion processes (Springer Science & Business Media, 2013)
44. A. DasGupta, Probability for statistics and machine learning: fundamentals and advanced topics (Springer Science & Business Media, 2011)
45. M. Ghosh, N. Mukhopadhyay, P.K. Sen, Sequential estimation, vol. 904 (John Wiley & Sons, 2011)
46. W. Whitt, Stochastic-process limits: an introduction to stochastic-process limits and their application to queues (Springer Science & Business Media, 2002)
47. C.E. Miles, S.D. Lawley, J.P. Keener, arXiv preprint arXiv:1711.04852 (2017)